

Supersymmetric $SO(10)$ -inspired leptogenesis and a new N_2 -dominated scenario

Pasquale Di Bari and Michele Re Fiorentin

*Physics and Astronomy, University of Southampton,
Southampton, SO17 1BJ, U.K.*

February 28, 2024

Abstract

We study the supersymmetric extension of $SO(10)$ -inspired thermal leptogenesis showing the constraints on neutrino parameters and on the reheat temperature T_{RH} that derive from the condition of successful leptogenesis from next-to-lightest right handed (RH) neutrinos (N_2) decays and the more stringent ones when independence of the initial conditions (strong thermal leptogenesis) is superimposed. In the latter case, the increase of the lightest right-handed neutrino (N_1) decay parameters helps the wash-out of a pre-existing asymmetry and constraints relax compared to the non-supersymmetric case. We find significant changes especially in the case of large $\tan \beta$ values ($\gtrsim 15$). In particular, for normal ordering, the atmospheric mixing angle can now be also maximal. The lightest left-handed neutrino mass is still constrained within the range $10 \lesssim m_1/\text{meV} \lesssim 30$ (corresponding to $75 \lesssim \sum_i m_i/\text{meV} \lesssim 120$). Inverted ordering is still disfavoured, but an allowed region satisfying strong thermal leptogenesis opens up at large $\tan \beta$ values. We also study in detail the lower bound on T_{RH} finding $T_{\text{RH}} \gtrsim 1 \times 10^{10} \text{ GeV}$ independently of the initial N_2 abundance. Finally, we propose a new N_2 -dominated scenario where the N_1 mass is lower than the sphaleron freeze-out temperature. In this case there is no N_1 wash-out and we find $T_{\text{RH}} \gtrsim 1 \times 10^9 \text{ GeV}$. These results indicate that $SO(10)$ -inspired thermal leptogenesis can be made compatible with the upper bound from the gravitino problem, an important result in light of the role often played by supersymmetry in the quest of a realistic model of fermion masses.

1 Introduction

There is no evidence so far of new physics at the electroweak scale or below, in particular not of the kind that would be required in order to address the problem of the matter-antimatter asymmetry of the Universe within the Standard Model.¹ On the other hand, the lightness of neutrino masses, within a minimal type I seesaw mechanism [1], would point to the existence of a very high energy scale intriguingly close to the grand-unified scale. This encourages the idea that the cosmological matter-antimatter asymmetry might have been generated in the early Universe well above the electro-weak energy scale. Traditional high energy leptogenesis [4] scenarios based on the minimal type I seesaw mechanism naturally realise this interpretation of the current phenomenological picture. However, testing these scenarios is challenging, relying on the possibility to find the way to over-constrain the large seesaw parameter space imposing successful leptogenesis within a definite model of new physics embedding the type I seesaw mechanism.

A traditional, and somehow paradigmatic, example of models able to embed the type I seesaw mechanism realising leptogenesis is given by $SO(10)$ -inspired models [5, 6]. In these models the fermion mass matrices, including the RH neutrino Majorana mass matrix, are not independent of each other but linked by relations that reduce the number of independent parameters establishing connections, for example between the quark and the lepton sector. In particular, the Dirac neutrino masses are typically not too different from the up quark masses. Moreover the mismatch between the flavour basis, where the charged lepton mass matrix is diagonal and the Yukawa basis, where the neutrino Dirac mass matrix is diagonal, can be described by a unitary matrix acting on the left-handed neutrino fields with mixing angles comparable to those of the CKM matrix in the quark sector.

$SO(10)$ -inspired relations are realised not only within traditional $SO(10)$ models [7] but, mentioning some recent examples, also within models combining grand-unification with discrete flavour symmetries [8] or with extra dimensions [9]. Barring fine tuned cancellations in the seesaw formula, the resulting RH neutrino mass spectrum would be highly hierarchical with the RH neutrino masses proportional to the squares of the up-quark masses with typical values $(M_1, M_2, M_3) \sim (10^5, 10^{11}, 10^{15})$ GeV. In this case the final asymmetry has to be necessarily dominantly produced by the N_2 decays, since the

¹The recent diphoton excess reported by the ATLAS and CMS collaborations [2], if confirmed, might or might not have direct relevance for baryogenesis. It might have if the excess is explained for example by a new scalar as predicted in the NMSSM that would be able to re-open electroweak baryogenesis viability [3]. Or, more indirectly, the excess could be associated to a new resonance signalling the existence of new strong dynamics that might originate within a grand-unified theory embedding leptogenesis.

contributions both from the N_1 and from the heaviest RH neutrinos (N_3) decays are too small to explain the observed value: an N_2 -dominated scenario of leptogenesis is therefore naturally realised [10]. It is interesting that this scenario necessarily requires the existence of at least three RH neutrino species in order for the N_2 CP asymmetries to get a sizeable contribution from the interference between tree level N_2 decays and one loop graphs with the exchange of virtual N_3 's. Therefore, there is an intriguing convergence between the $SO(10)$ prediction for the existence of three RH neutrino species and the requirements of N_2 -dominated leptogenesis.

A challenging crucial aspect of this scenario is the necessity for the asymmetry produced by the N_2 decays to survive the N_1 wash-out. Flavour effects [11, 12, 13] greatly enhance the region in the space of parameters where the N_1 wash-out is negligible since this acts separately on the three charged lepton flavours [14, 15]. In this way it has been shown that flavour effects indeed rescue $SO(10)$ -inspired models with strong hierarchical RH neutrino spectrum [16]. Interestingly, imposing successful $SO(10)$ -inspired leptogenesis one obtains constraints on low energy neutrino parameters that can be testable [17]. These have been also derived and explained analytically in the approximation where the mismatch between the flavour and the Yukawa basis is neglected [18]. In particular the lightest left-handed (LH) neutrino mass is constrained within the range $1\text{ meV} \lesssim m_1 \lesssim 300\text{ meV}$. The upper bound ² has now been tested by latest cosmological results that place an upper bound on the sum of the neutrino masses $\sum_i m_i \lesssim 0.23\text{ eV}$ [21], translating into $m_1 \lesssim 70\text{ meV}$. ³

Another interesting constraint is placed on the atmospheric mixing angle. This has to be necessarily in the second octant in the case of inverted ordered (IO) neutrino masses. More stringent constraints on the low energy neutrino parameters can be obtained superimposing additional conditions. An interesting possibility is to impose the so called *strong thermal condition*, the requirement that the asymmetry is independent of the initial conditions. This is indeed nicely realised within $SO(10)$ -inspired models [22] and results into a ‘strong thermal $SO(10)$ -inspired solution’ characterized by normally ordered (NO) neutrino masses, lightest neutrino mass in the range $10\text{ meV} \lesssim m_1 \lesssim 30\text{ meV}$, atmospheric mixing angle in the first octant and Dirac phase $\delta \sim -45^\circ$, in very nice agreement with current best fit results from neutrino oscillation experiments global analyses [23].

Recently it has been shown that flavour coupling [11, 24, 25, 12] can help to open new

²Notice that this is more relaxed compared to the upper bound holding in the N_1 dominated scenario where $m_1 \lesssim 0.1\text{ eV}$ [19, 20, 15].

³Future cosmological observations should be able to constraint $m_1 \gtrsim 10\text{ meV}$ at 95% C.L. and in this case they would test most of the window allowed by $SO(10)$ -inspired leptogenesis.

solutions [26] and these can be crucial to realise successful leptogenesis within specific models. An explicit example has been recently obtained in [27] within a specific realistic grand unified model, the ‘A to Z model’ [8], obtaining quite definite predictions on the atmospheric mixing angle ($\theta_{23} \sim 52^\circ$), Dirac phase ($\delta \sim 20^\circ$) and on the ordering (NO). Alternatively, at the expense of very highly fine tuned seesaw cancellations, in the vicinity of a crossing level solutions one can have a departure from a very highly hierarchical pattern [6] in a way that M_1 can be uplifted and its CP asymmetry strongly enhanced. Recently this kind of solution has been realised within a realistic fit of quark and neutrino parameters within $SO(10)$ models. In this case the uplift of M_1 is also accompanied by a simultaneous decrease of M_3 so that a compact spectrum is obtained [28] and this can also lead to successful leptogenesis [29]. An unpleasant feature of these solutions, in addition to the very high fine tuning, is that, because of the uplift of M_1 , they predict NO and too small values for the neutrinoless double beta decay effective neutrino mass m_{ee} to be measured [18].

Supersymmetric extensions of $SO(10)$ -models are important since they offer a traditional way to address naturalness. At the same time they help improving the goodness of fits of lepton and quark parameters [30, 28]. Recently [28] good fits of the fermion parameters have been obtained within $SO(10)$ models with hierarchical RH neutrino masses and interestingly IO light neutrino masses, leading to values of m_{ee} well in the reach of next generation neutrinoless double beta decay experiments. However, supersymmetry is typically implemented as a local symmetry leading to supergravity and in this case one has to worry whether successful thermal leptogenesis can be achieved with values of T_{RH} compatible with the upper bound from the solution of the gravitino problem [31]. A quite conservative model independent upper bound, $T_{RH} \lesssim 10^{10}$ GeV, comes from preventing Dark Matter over abundance, where the Dark Matter particle can be either the neutralino or the gravitino itself or some other hidden sector lighter particle depending whether the gravitino is or it is not the lightest supersymmetric particle.⁴

In this paper we extend the study of $SO(10)$ -inspired leptogenesis to the supersymmetric case, showing how the constraints derived in the non-supersymmetric case change, with a particular focus on the lower bound on T_{RH} . We find that in a traditional scenario, where the lightest RH neutrino wash-out has to be taken into account, this can be as low

⁴It should be noticed, however, that different ways to circumvent even this upper bound have been proposed. For example thanks to entropy production diluting Dark Matter abundance [32] or in models with mixed axion/axino Dark Matter [33] or yet another way to evade completely this upper bound is that the gravitino is heavier than $\sim 10^7$ GeV in a way that its life-time is so short to decay before neutralino dark matter freeze-out [34].

as $\sim 10^{10}$ GeV or even below admitting some fine tuning in the seesaw parameters and an initial thermal N_2 abundance. These results indicate that, in those supersymmetric scenarios where the gravitino is heavier than ~ 30 TeV and decays prior to the onset of BBN, $SO(10)$ -inspired thermal leptogenesis can be indeed reconciled with the gravitino problem. Similar analysis, though for more specific choices of the parameters, has been also done in [35], finding a much more stringent lower bound $T_{\text{RH}} \gtrsim 5 \times 10^{11}$ GeV and concluding that thermal $SO(10)$ -inspired leptogenesis is incompatible with the upper bound from the gravitino problem thus motivating a non-thermal scenario. We will comment on this difference between our results and those of [35].

We also propose a new scenario where the lightest RH neutrino mass is comparable or below the sphaleron freeze-out temperature $T_{\text{sph}}^{\text{out}} \sim 100$ GeV [36] in a way that the lightest RH neutrino wash-out occurs too late to wash-out the baryon asymmetry. In this case we show that values of T_{RH} as low as $\sim 10^9$ GeV are possible. Therefore, our results indicate that supersymmetric $SO(10)$ -inspired thermal leptogenesis can be reconciled with the gravitino problem and is certainly not ruled out model independently.

The paper is organised in the following way. In Section 2 we show how the calculation of the asymmetry can be extended to a supersymmetric N_2 -dominated scenario. In Section 3 we study $SO(10)$ -inspired (supersymmetric) leptogenesis deriving the constraints on the low energy neutrino parameters and comparing them with those obtained in the non-supersymmetric case in [17, 22, 18]. In Section 4 we discuss in detail the lower bound on T_{RH} showing that values as low as $\simeq 1 \times 10^{10}$ GeV are possible. In Section 5 we discuss a new N_2 -dominated scenario where the lightest RH neutrino mass is lower than the sphaleron freeze out temperature, so that the N_1 wash-out is absent. We recalculate the lower bound on T_{RH} in this scenario obtaining $T_{\text{RH}} \gtrsim 1 \times 10^9$ GeV, enlarging even more the region of compatibility with the gravitino problem. In Section 6 we draw some final remarks and conclude.

2 Calculation of the asymmetry within supersymmetric N_2 -dominated leptogenesis

In this section we extend the calculation of the asymmetry in the N_2 -dominated scenario, as rising from $SO(10)$ -inspired conditions, to a supersymmetric framework.

First of all we assume a minimal type I seesaw extension of the MSSM introducing three RH neutrinos N_{iR} with Yukawa couplings h and Majorana mass M . In the flavour basis, where the charged lepton and the Majorana mass matrices are both diagonal, the

masses and Yukawa couplings relevant for leptogenesis are given by the following terms in the superpotential [37, 38] ($\alpha = e, \mu, \tau$)

$$\mathcal{W}_{\ell+\nu+N} = \overline{\alpha_L} \epsilon H_d D_{h_\ell} \alpha_R + H_u \epsilon \overline{\nu_{\alpha L}} h_{\nu\alpha i} N_{iR} + \frac{1}{2} \overline{N_{iR}^c} D_M N_{iR} + \text{h.c.}, \quad (1)$$

where $D_{h_\ell} \equiv \text{diag}(h_e, h_\mu, h_\tau)$, $D_M \equiv \text{diag}(M_1, M_2, M_3)$, with $M_1 \leq M_2 \leq M_3$, and ϵ is the totally anti-symmetric tensor.

After spontaneous symmetry breaking the two neutral Higgs field vev's generate the Dirac masses for the charged leptons and for the neutrinos, respectively

$$m_\ell = v_d h_\ell \quad \text{and} \quad m_D = v_u h_\nu, \quad (2)$$

with $\tan \beta \equiv v_u/v_d$ and $v = \sqrt{v_u^2 + v_d^2} \simeq 174.6 \text{ GeV}$, where v is the SM Higgs vev. The Dirac mass matrix in the flavour basis can be expressed through the singular value decomposition (or bi-unitary parameterisation) as

$$m_D = V_L^\dagger D_{m_D} U_R, \quad (3)$$

where $D_{m_D} \equiv \text{diag}(m_{D1}, m_{D2}, m_{D3})$ is the neutrino Dirac mass matrix in the Yukawa basis and V_L and U_R are the unitary matrices acting respectively on the LH and RH neutrino fields in the transformation from the flavour basis to the Yukawa basis.

In the seesaw limit, for $M \gg m_D$, the spectrum of neutrino mass eigenstates splits into a very heavy set with masses almost coinciding with the Majorana masses M_i and into a light set $\nu_i \simeq \nu_{iL} + \nu_{iL}^c$, with a symmetric mass matrix m_ν given by the seesaw formula

$$m_\nu = -m_D \frac{1}{D_M} m_D^T. \quad (4)$$

This is diagonalised by a unitary matrix U ,

$$U^\dagger m_\nu U^\star = -D_m, \quad (5)$$

where $D_m \equiv \text{diag}(m_1, m_2, m_3)$ with $m_1 \leq m_2 \leq m_3$, corresponding to the PMNS leptonic mixing matrix, in a way that we can write

$$D_m = U^\dagger m_D \frac{1}{D_M} m_D^T U^\star. \quad (6)$$

Assuming $SO(10)$ -inspired conditions, i) $I \leq V_L \leq V_{CKM}$ and ii) $\alpha_i \equiv m_{Di}/m_{q_i} = \mathcal{O}(0.1-10)$, where m_{q_i} are the three up quark masses, m_u , m_c and m_t for $i = 1, 2, 3$ respectively, the RH neutrino masses are approximated by the following simple analytical expressions [6, 18, 27]

$$M_1 \simeq \frac{(m_{D1})^2}{|(\tilde{m}_\nu)_{11}|}, \quad M_2 \simeq \frac{(m_{D2})^2 |(\tilde{m}_\nu)_{11}|}{m_1 m_2 m_3 |(\tilde{m}_\nu^{-1})_{33}|}, \quad M_3 \simeq (m_{D3})^2 |(\tilde{m}_\nu^{-1})_{33}|, \quad (7)$$

where $\tilde{m}_\nu \equiv V_L m_\nu V_L^T$ is the light neutrino mass matrix in the Yukawa basis. These expressions show that under $SO(10)$ -inspired conditions, barring fine tuned conditions on $(\tilde{m}_\nu)_{11}$ and $(\tilde{m}_\nu^{-1})_{33}$ ⁵, the RH neutrino masses are highly hierarchical and in particular $M_1 \ll 10^9 \text{ GeV}$ and $M_2 \gg 10^9 \text{ GeV}$, in a way that the N_2 -dominated scenario is realised, where the asymmetry is necessarily produced by the N_2 's.

A general calculation of the asymmetry valid for any mass regime should proceed within a density matrix formalism [11, 13, 39, 40]. However, except for some transition regimes, the mass of the N_2 producing the asymmetry, M_2 , falls within so called fully flavoured regimes where the density matrix equation simplifies into Boltzmann equations [40] and in this case the final asymmetry can be calculated using simple approximate analytic expressions.

We will neglect flavour coupling effects [11, 12, 25, 26], that can in some cases produce dominant contributions to the final asymmetry [26, 27] and have been studied in detail in the supersymmetric case in [41], but we will comment in the conclusions on the impact they can have on our results. We will also not pursue here the case of soft leptogenesis, offering a way to lower the scale of leptogenesis circumventing the gravitino problem [42].

It is important to notice that, within a supersymmetric framework, the N_2 -production of the asymmetry for a fixed mass M_2 can occur in different fully flavoured regimes depending on the value of $\tan \beta$ since charged lepton interaction rates involving leptons are $\propto (1 + \tan^2 \beta)$ [12]. On the other hand since, because of our working assumptions, one has $M_1 \ll 10^9 \text{ GeV}$, the lightest RH neutrino produced asymmetry is always negligible and the N_1 wash-out occurs always in the three-flavoured regime independently of the value of $\tan \beta$. We can then distinguish three fully flavoured regimes for the calculation of the asymmetry:

- In the unflavoured⁶ regime, for $M_2 \gg 5 \times 10^{11} \text{ GeV} (1 + \tan^2 \beta)$, the final $B - L$ asymmetry can be calculated using

$$\begin{aligned} N_{B-L}^f &\simeq \left[\frac{K_{2e}}{K_2} \varepsilon_2 \kappa(K_2) + \left(\varepsilon_{2e} - \frac{K_{2e}}{K_2} \varepsilon_2 \right) \kappa(K_2/2) \right] e^{-\frac{3\pi}{8} K_{1e}} \\ &+ \left[\frac{K_{2\mu}}{K_2} \varepsilon_2 \kappa(K_2) + \left(\varepsilon_{2\mu} - \frac{K_{2\mu}}{K_2} \varepsilon_2 \right) \kappa(K_2/2) \right] e^{-\frac{3\pi}{8} K_{1\mu}} \\ &+ \left[\frac{K_{2\tau}}{K_2} \varepsilon_2 \kappa(K_2) + \left(\varepsilon_{2\tau} - \frac{K_{2\tau}}{K_2} \varepsilon_2 \right) \kappa(K_2/2) \right] e^{-\frac{3\pi}{8} K_{1\tau}}. \end{aligned} \quad (8)$$

⁵Recently it has been noticed that such a fine tuning can be precisely quantified in terms of the orthogonal matrix [27].

⁶Here we refer to an ‘unflavoured’ regime rather than to a ‘one-flavoured’ regime, as sometimes it is done, since we refer only to the number of charged lepton flavours.

- In the two-(fully) flavoured regime, for $5 \times 10^{11} \text{ GeV} (1 + \tan^2 \beta) \gg M_2 \gg 5 \times 10^8 \text{ GeV} (1 + \tan^2 \beta)$, the final $B - L$ asymmetry can be calculated using

$$\begin{aligned}
N_{B-L}^f &\simeq \left[\frac{K_{2e}}{K_{2\tau_2^\perp}} \varepsilon_{2\tau_2^\perp} \kappa(K_{2\tau_2^\perp}) + \left(\varepsilon_{2e} - \frac{K_{2e}}{K_{2\tau_2^\perp}} \varepsilon_{2\tau_2^\perp} \right) \kappa(K_{2\tau_2^\perp}/2) \right] e^{-\frac{3\pi}{8} K_{1e}} + \\
&+ \left[\frac{K_{2\mu}}{K_{2\tau_2^\perp}} \varepsilon_{2\tau_2^\perp} \kappa(K_{2\tau_2^\perp}) + \left(\varepsilon_{2\mu} - \frac{K_{2\mu}}{K_{2\tau_2^\perp}} \varepsilon_{2\tau_2^\perp} \right) \kappa(K_{2\tau_2^\perp}/2) \right] e^{-\frac{3\pi}{8} K_{1\mu}} + \\
&+ \varepsilon_{2\tau} \kappa(K_{2\tau}) e^{-\frac{3\pi}{8} K_{1\tau}}, \tag{9}
\end{aligned}$$

where we indicated with τ_2^\perp the electron plus muon component of the quantum flavour states produced by the N_2 -decays defining $K_{2\tau_2^\perp} \equiv K_{2e} + K_{2\mu}$, $\varepsilon_{2\tau_2^\perp} \equiv \varepsilon_{2e} + \varepsilon_{2\mu}$.

- Finally, in the three-flavoured regime, for $M_2 \ll 5 \times 10^8 \text{ GeV} (1 + \tan^2 \beta)$, the final $B - L$ asymmetry can be calculated using

$$N_{B-L}^f \simeq \varepsilon_{2e} \kappa(K_{2e}) e^{-\frac{3\pi}{8} K_{1e}} + \varepsilon_{2\mu} \kappa(K_{2\mu}) e^{-\frac{3\pi}{8} K_{1\mu}} + \varepsilon_{2\tau} \kappa(K_{2\tau}) e^{-\frac{3\pi}{8} K_{1\tau}}. \tag{10}$$

As we discussed, in the transition regimes, about $M_2 \sim 5 \times 10^{11} \text{ GeV} (1 + \tan^2 \beta)$ and $M_2 \sim 5 \times 10^8 \text{ GeV} (1 + \tan^2 \beta)$, the asymmetry should be calculated using density matrix equations. We will describe these transition regimes switching abruptly from one fully flavoured regime to another at the two given values of M_2 . We will also comment on the impact of this ‘step approximation’.

The total and flavoured decay parameters, K_i and $K_{i\alpha}$ respectively, can be still written as

$$K_{i\alpha} \equiv \frac{\Gamma(T=0)}{H(T=M_i)} = \frac{|m_{D\alpha i}|^2}{m_\star^{MSSM} M_i} \quad \text{and} \quad K_i = \sum_\alpha K_{i\alpha} = \frac{(m_D^\dagger m_D)_{ii}}{m_\star^{MSSM} M_i}, \tag{11}$$

but the equilibrium neutrino mass is now given by [43, 35]

$$m_\star^{MSSM} \equiv \frac{8 \pi^{5/2} \sqrt{g_\star^{MSSM}}}{3 \sqrt{5}} \frac{v_u^2}{M_{Pl}} = \frac{1}{2} \sqrt{\frac{g_\star^{MSSM}}{g_\star^{SM}}} m_\star^{SM} \sin^2 \beta \simeq 0.78 \times 10^{-3} \text{ eV} \sin^2 \beta, \tag{12}$$

having taken into account that: i) RH neutrinos and sneutrinos have a doubled number of decay channels compared to the SM case that simply doubles the rates and ii) the number of ultra-relativistic degrees of freedom $g_\star^{MSSM} = 915/4$. This implies that the (total and flavoured) decay parameters are $\sim \sqrt{2}$ larger than in the SM.⁷ This will clearly tend to enhance the wash-out both at the production, depending on the $K_{2\alpha}$ ’s, and from

⁷We will assume that the number of ultra-relativistic degrees of freedom stays constant between N_2 production at $T \sim M_2$ and N_1 wash-out occurring at $T \sim M_1$. However, in general one can think of

the lightest RH neutrinos, depending on the $K_{1\alpha}$'s. The wash-out at the production is described by the efficiency factor $\kappa(K_{2\alpha})$ that for an initial thermal N_2 abundance can be calculated as [20, 44]

$$\kappa(K_{2\alpha}) = \frac{2}{z_B(K_{2\alpha}) K_{2\alpha}} \left(1 - e^{-\frac{K_{2\alpha} z_B(K_{2\alpha})}{2}} \right), \quad z_B(K_{2\alpha}) \simeq 2 + 4 K_{2\alpha}^{0.13} e^{-\frac{2.5}{K_{2\alpha}}}. \quad (13)$$

For an initial vanishing N_2 abundance this is the sum of a negative and a positive contribution [20],

$$\kappa(K_{2\alpha}, K_2) = \kappa_-^f(K_2, K_{2\alpha}) + \kappa_+^f(K_2, K_{2\alpha}), \quad (14)$$

that are approximated by the following expressions [44]

$$\kappa_-^f(K_2, K_{2\alpha}) \simeq -\frac{2}{p_{2\alpha}^0} e^{-\frac{3\pi}{8} K_{2\alpha}} \left(e^{\frac{p_{2\alpha}^0}{2} \bar{N}(K_2)} - 1 \right) \quad (15)$$

and

$$\kappa_+^f(K_2, K_{2\alpha}) \simeq \frac{2}{z_B(K_{2\alpha}) K_{2\alpha}} \left(1 - e^{-\frac{K_{2\alpha} z_B(K_{2\alpha}) \bar{N}(K_2)}{2}} \right), \quad (16)$$

where

$$\bar{N}(K_2) \equiv \frac{N(K_2)}{\left(1 + \sqrt{N(K_2)} \right)^2}, \quad (17)$$

and $p_{2\alpha}^0 = K_{2\alpha}/K_2$ is the tree level probability that the lepton quantum state produced by a N_2 -decay is measured as an α flavour eigenstate. If the asymmetry is produced in the strong wash-out regime, the two expressions converge to the same asymptotic limit and there is no dependence on the initial N_2 abundance.

The other important modification to be taken into account, compared to the non-supersymmetric case, is that now there are also more interference terms contributing to the CP asymmetries and one obtains [37]

$$\varepsilon_{2\alpha} = \frac{3}{8\pi} \frac{M_2 m_{\text{atm}}}{v^2} \sum_{j \neq 2} \left(\mathcal{I}_{2j}^\alpha \xi(M_j^2/M_2^2) + \frac{2}{3} \mathcal{J}_{2j}^\alpha \frac{M_j/M_2}{M_j^2/M_2^2 - 1} \right), \quad (18)$$

where we defined [45],

$$\mathcal{I}_{2j}^\alpha \equiv \frac{\text{Im}[(m_D^\dagger)_{i\alpha} (m_D)_{\alpha j} (m_D^\dagger m_D)_{ij}]}{M_2 M_j \tilde{m}_2 m_{\text{atm}}}, \quad \mathcal{J}_{2j}^\alpha \equiv \frac{\text{Im}[(m_D^\dagger)_{i\alpha} (m_D)_{\alpha j} (m_D^\dagger m_D)_{ji}]}{M_2 M_j \tilde{m}_2 m_{\text{atm}}}, \quad (19)$$

(model dependent) supersymmetric models where M_1 is low enough that some supersymmetric degrees of freedom associate to heavier particles get suppressed in between. In Section 5 we will consider a scenario with $M_1 \lesssim 100 \text{ GeV}$ but in that case we will point out that the N_1 wash-out at all can be neglected so in any case this point has no relevance.

with $\tilde{m}_2 \equiv (m_D^\dagger m_D)_{22}/M_2$, and

$$\xi(x) = \frac{x}{3} \left[\ln \left(\frac{1+x}{x} \right) - \frac{2}{1-x} \right]. \quad (20)$$

In the hierarchical RH neutrino mass limit one has $\xi(x) \rightarrow 1$ and moreover terms $\propto \mathcal{I}_{21}^\alpha \xi(M_1^2/M_2^2)$, \mathcal{J}_{21}^α , \mathcal{J}_{23}^α are strongly suppressed in the N_2 -dominated scenario so that the $\varepsilon_{2\alpha}$'s can be approximated simply by

$$\varepsilon_{2\alpha} \simeq \frac{3}{8\pi} \frac{M_2 m_{\text{atm}}}{v^2} \mathcal{I}_{23}^\alpha. \quad (21)$$

Compared to the SM case, for a given set of values of the seesaw parameters, the CP asymmetries are double. Finally the baryon-to-photon number ratio can be calculated from the final $B - L$ asymmetry produced by the RH neutrinos (or sneutrinos), as $\eta_B \simeq d^{MSSM} N_{B-L}^f$, where [43]

$$d^{MSSM} = 2 \left(\frac{a_{\text{sph}}}{N_\gamma^{\text{rec}}} \right)^{MSSM} \simeq 0.89 \times 10^{-2} \simeq 0.92 d^{SM}, \quad (22)$$

having taken into account a factor 2 from the sum of the asymmetry generated by RH neutrinos and sneutrinos, the sphaleron conversion coefficient $a_{\text{sph}}^{MSSM} = 8/23$ [46] and that the number of photons at recombination is given by $(N_\gamma^{\text{rec}})^{MSSM} = 4 g_\star^{MSSM} / (3 g_\star^{\text{rec}}) \simeq 78$ since $g_\star^{MSSM} = 915/4$, $g_\star^{\text{rec}} \simeq 3.91$ and one has to consider that in the portion of co-moving volume containing one RH neutrino in ultra-relativistic equilibrium there are 4/3 photons.

In the non supersymmetric case, and in the approximation $V_L \simeq I$, the solutions are tauon dominated [16] and, as shown in [18], the asymmetry is well described by a full analytical expression. We can extend this analytical expression, for the tauon contribution to the final asymmetry, to the supersymmetric case with the simple modifications we discussed ⁸, obtaining

$$\begin{aligned} N_{B-L}^f|_{V_L=I} &\simeq \frac{3}{8\pi} \frac{\alpha_2^2 m_c^2}{v^2} \frac{|m_{\nu ee}| (|(m_\nu^{-1})_{\tau\tau}|^2 + |(m_\nu^{-1})_{\mu\tau}|^2)^{-1}}{m_1 m_2 m_3} \frac{|(m_\nu^{-1})_{\mu\tau}|^2}{|(m_\nu^{-1})_{\tau\tau}|^2} \sin \alpha_L \quad (23) \\ &\times \kappa \left(\frac{m_1 m_2 m_3}{m_\star} \frac{|(m_\nu^{-1})_{\mu\tau}|^2}{|m_{\nu ee}| |(m_\nu^{-1})_{\tau\tau}|} \right) \\ &\times e^{-\frac{3\pi}{8} \frac{|m_{\nu e\tau}|^2}{m_\star |m_{\nu ee}|}}, \end{aligned}$$

with

$$\alpha_L = \text{Arg}[m_{\nu ee}] - 2 \text{Arg}[(m_\nu^{-1})_{\mu\tau}] + \pi - 2(\rho + \sigma). \quad (24)$$

⁸In addition we are correcting a typo that we found in [18] where instead of the term $|m_\nu^{-1})_{\mu\tau}|^2/|(m_\nu^{-1})_{\tau\tau}|^2$ there is, incorrectly, its inverse.

We will have of course to check whether the tau dominance, holding for $V_L = I$ in the non-supersymmetric case, still holds in the supersymmetric case.

Finally, we also want to give the expression for the relic value of a pre-existing asymmetry and the condition for its wash-out (strong thermal leptogenesis condition) that we will superimpose to the successful leptogenesis condition, extending the results found in the non-supersymmetric case [22].

If the production occurs in the unflavoured regime, for $M_2 \gg 5 \times 10^{11} \text{ GeV} (1 + \tan^2 \beta)$, then it is impossible to realise successful strong thermal leptogenesis since the N_2 wash-out cannot suppress completely the pre-existing asymmetry in any of the three (charged lepton) flavours. The pre-existing asymmetry can be only washed-out by the lightest RH neutrinos in all three flavours [47] but in this way it also suppresses the N_2 produced asymmetry and one cannot attain successful leptogenesis. On the other hand if the N_2 production occurs in the two fully-flavoured regime, for $5 \times 10^{11} \text{ GeV} (1 + \tan^2 \beta) \gg M_2 \gg 5 \times 10^8 \text{ GeV} (1 + \tan^2 \beta)$, then the relic value of the pre-existing $B - L$ asymmetry is given by

$$N_{B-L}^{\text{p,f}} = N_{\Delta_\tau}^{\text{p,f}} + N_{\Delta_\mu}^{\text{p,f}} + N_{\Delta_e}^{\text{p,f}}, \quad (25)$$

where

$$\begin{aligned} N_{\Delta_\tau}^{\text{p,f}} &= p_{\text{p}\tau}^0 e^{-\frac{3\pi}{8}(K_{1\tau}+K_{2\tau})} N_{B-L}^{\text{p,i}}, \\ N_{\Delta_\mu}^{\text{p,f}} &= (1 - p_{\text{p}\tau}^0) e^{-\frac{3\pi}{8}K_{1\mu}} \left[p_{\mu\tau_2^\perp}^0 p_{\text{p}\tau_2^\perp}^0 e^{-\frac{3\pi}{8}(K_{2e}+K_{2\mu})} + (1 - p_{\mu\tau_2^\perp}^0)(1 - p_{\text{p}\tau_2^\perp}^0) \right] N_{B-L}^{\text{p,i}}, \\ N_{\Delta_e}^{\text{p,f}} &= (1 - p_{\text{p}\tau}^0) e^{-\frac{3\pi}{8}K_{1e}} \left[p_{e\tau_2^\perp}^0 p_{\text{p}\tau_2^\perp}^0 e^{-\frac{3\pi}{8}(K_{2e}+K_{2\mu})} + (1 - p_{e\tau_2^\perp}^0)(1 - p_{\text{p}\tau_2^\perp}^0) \right] N_{B-L}^{\text{p,i}}. \end{aligned} \quad (26)$$

In this case imposing $K_{2\tau}, K_{1\mu}, K_{1e} \gg 1$ and $K_{1\tau} \lesssim 1$ one can wash-out the pre-existing asymmetry but not the tauonic component of the N_2 produced asymmetry [48]. This is the case holding in the non-supersymmetric case or in the supersymmetric case for small $\tan \beta$ values. On the other hand for sufficiently large $\tan \beta$ values, such that $M_2 \ll 5 \times 10^8 \text{ GeV} (1 + \tan^2 \beta)$, the production occurs in the three-flavoured regime and in this case the relic value of the final flavoured asymmetries are simply modified by the replacement $K_{1\mu} \rightarrow K_{1\mu} + K_{2\mu}$ and $K_{1e} \rightarrow K_{1e} + K_{2e}$ in the exponentials. In this way the conditions for the wash-out of the pre-existing asymmetry are now less stringent since one has to impose $K_{2\tau}, K_{1\mu} + K_{2\mu}, K_{1e} + K_{2e} \gg 1$, so that one can also have $K_{2\mu} \gg 1$ and $K_{1\mu} \lesssim 1$, washing-out the pre-existing asymmetry and having a final muon (instead of tauon) dominated asymmetry, a new situation compared to the non-supersymmetric case.

3 Constraints on the low energy neutrino parameters

In the $SO(10)$ -inspired scenario of leptogenesis that we described, the asymmetry formally depends on the nine parameters in the low energy neutrino mass matrix, on the six parameters in the matrix V_L and on the three α_i . As we discussed the 3 RH neutrino masses M_i and the RH neutrino mixing matrix U_R can be expressed in terms of these parameters. However, since the final asymmetry is dominated by the N_2 contribution, the dependence on α_1 and α_3 cancels out (this can be seen analytically in the eq. (23) for $V_L = I$ but the result remains true for a generic V_L) and this is crucial to understand why one gets constraints on the low energy neutrino parameters.

We have numerically calculated the final asymmetry and imposed the condition of successful leptogenesis in the $SO(10)$ -inspired case producing scatter plots in the space of parameters for $(\alpha_1, \alpha_2, \alpha_3) = (1, 5, 1)$. As in [16, 17, 18], for the up quark masses at the leptogenesis scale we adopted the values $m_u = 1$ MeV, $m_c = 400$ MeV and $m_t = 100$ GeV [49]. We verified that indeed constraints do not depend on α_1 and α_3 but only on α_2 as in the non-supersymmetric case [17].⁹ The value $\alpha_2 = 5$ can be considered a close-to-maximum value in a way that the constraints obtained for this value have to be regarded close to the most conservative ones. Moreover this value has been used as a benchmark value both in the non-supersymmetric case [16, 17] and also in [35], allowing us a useful comparison among the results.

We have to distinguish ‘small $\tan \beta$ values’ for which the production, as in the non-supersymmetric case, occurs in the two-flavoured regime, from ‘large $\tan \beta$ values’, for which the production occurs in the three-flavoured regime. Since for successful $SO(10)$ -inspired leptogenesis one typically has $M_2 \gtrsim 10^{11}$ GeV and since the transition from the two to the three flavoured regime occurs for $M_2 \simeq 5 \times 10^8 \text{ GeV}(1 + \tan^2 \beta)$, one can say that for $\tan \beta \gtrsim 15$ the production occurs mainly in the three flavoured regime, while for $\tan \beta \lesssim 15$ it occurs mainly in the two-flavoured regime. We made the calculation for two extreme values, $\tan \beta = 5$ and $\tan \beta = 50$. In the first case the production occurs almost entirely in the two flavoured regime, except for very special points, while in the second case the production occurs mostly in the three flavoured regime.

We also performed the scatter plots both for NO and for IO neutrino masses so that in total we have four cases to consider.

In addition to successful leptogenesis, we also show the results when the condition of strong thermal leptogenesis, such that a large pre-existing asymmetry is washed-out, is

⁹This statement is true under the implicit assumption that α_1 is not that large that M_1 becomes larger than 10^9 GeV or α_3 that small to make $M_3/M_2 \lesssim 2$.

superimposed. As in the non-supersymmetric case [22], this singles out a sub set of the solutions out of those satisfying successful leptogenesis. In the scatter plots we highlight these sub sets in blue (light blue for $V_L = I$ and dark blue for $I \leq V_L \leq V_{CKM}$).

For the low energy neutrino parameters we adopted the same values and ranges as in [18]. In particular for the solar neutrino mass scale $m_{\text{sol}} \equiv \sqrt{m_2^2 - m_1^2} = 0.0087 \text{ eV}$ and for the atmospheric neutrino mass scale $m_{\text{atm}} \equiv \sqrt{m_3^2 - m_1^2} = 0.0495 \text{ eV}$, the best fit values found in a recent global analysis [23]. When these values are combined with the upper bound on the sum of the neutrino masses from the *Planck* satellite, $\sum_i m_i < 0.23 \text{ eV}$ (95% C.L.) [21], one obtains an upper bound on the lightest neutrino mass

$$m_1 \lesssim 0.07 \text{ eV}. \quad (27)$$

The mixing angles, respectively the reactor, the solar and the atmospheric ones, are now measured with the following best fit values and 1σ (3σ) ranges [50] for NO and IO respectively,

$$\begin{aligned} \theta_{13} &= 8.8^\circ \pm 0.4^\circ \quad (7.6^\circ\text{--}9.9^\circ) \quad \text{and} \quad \theta_{13} = 8.9^\circ \pm 0.4^\circ \quad (7.7^\circ\text{--}9.9^\circ), \\ \theta_{12} &= 33.7^\circ \pm 1.1^\circ \quad (30.6^\circ\text{--}36.8^\circ) \quad \text{and} \quad \theta_{12} = 33.7^\circ \pm 1.1^\circ \quad (30.6^\circ\text{--}36.8^\circ), \\ \theta_{23} &= 41.4^{+1.9^\circ}_{-1.4^\circ} \quad (37.7^\circ\text{--}52.3^\circ) \quad \text{and} \quad \theta_{23} = 42.4^{+8.0^\circ}_{-1.8^\circ} \quad (38.1^\circ\text{--}52.3^\circ). \end{aligned} \quad (28)$$

Current experimental data also start to put constraints on the Dirac phase and the following best fit values and 1σ errors are found for NO and IO respectively,

$$\delta/\pi = -0.61^{+0.38}_{-0.27} \quad \text{and} \quad \delta/\pi = -0.69^{+0.29}_{-0.33}, \quad (29)$$

though all values $[-\pi, +\pi]$ are still allowed at 3σ . They do not yet favour one of the two orderings over the other.

3.1 Normal ordering

Let us first present the results for NO neutrino masses. As mentioned, we also discuss separately the results for ‘low $\tan\beta$ ’ values and for ‘high $\tan\beta$ values’.

3.1.1 Small $\tan\beta$ values ($\tan\beta = 5$)

Let us first start discussing the results for $\tan\beta = 5$. As mentioned, this is a sufficiently low value for most of the allowed values of M_2 to fall in the two fully flavoured regime. The results are shown in Fig. 1. The yellow points are all those solutions realising successful $SO(10)$ -inspired leptogenesis for $I \leq V_L \leq V_{CKM}$ and initial thermal N_2 abundance. The

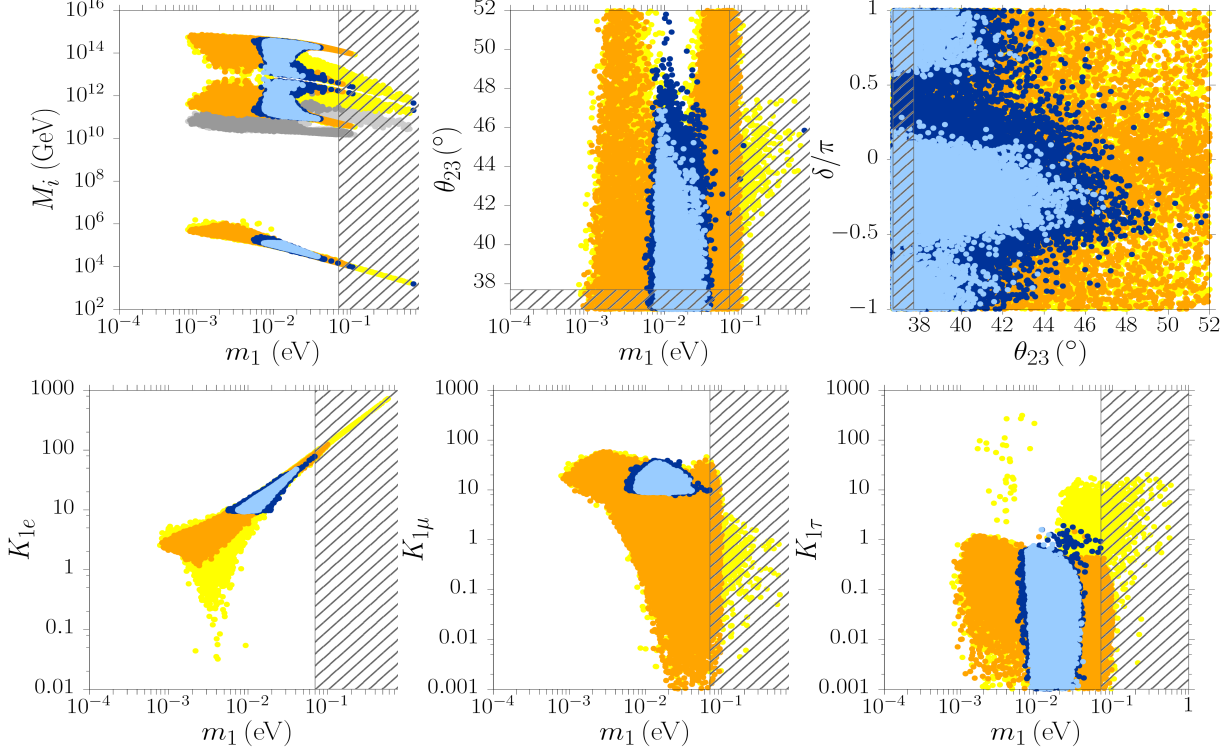


Figure 1: Scatter plots in the low energy neutrino parameter space projected on different selected planes for NO, $(\alpha_1, \alpha_2, \alpha_3) = (1, 5, 1)$, $M_3/M_2 > 3$, $\tan \beta = 5$ and initial thermal N_2 abundance. The yellow (orange) points respect the successful leptogenesis condition $\eta_B^{\text{lep}} > \eta_B^{\text{CMB}} > 5.9 \times 10^{-10}$ for $I \leq V_L \leq V_{\text{CKM}}$ ($V_L = I$) where η_B^{lep} is calculated from the eqs. (8), (9) and (10) depending on the value of M_2 determining the flavoured regime (mainly the two fully-flavoured regime) using a numerical determination of RH neutrino masses, mixing matrix and phases. The mixing angles vary within the 3σ ranges in Eqs. (28). The dark (light) blu points are those respecting the additional *strong thermal condition* for $I \leq V_L \leq V_{\text{CKM}}$ ($V_L = I$) for an initial value of the pre-existing asymmetry $N_{B-L}^{\text{p,i}} = 10^{-3}$. The dashed regions indicate either the values of m_1 excluded by the *Planck* upper bound $m_1 \lesssim 70$ meV (cf. eq. (27)) or the values of θ_{23} excluded by current data at 3σ (cf. eq. (28)). The grey points indicate the minimum value of T_{RH} .

orange points are the subset for $V_L = I$. These results for $\tan \beta = 5$ are similar to those obtained in the non-supersymmetric case and they are well explained and understood [16, 17, 18]. Even though they have been obtained for initial thermal N_2 abundance, they are actually very marginally dependent of the initial N_2 abundance since for the tauon-dominated solutions ($K_{1\tau} \lesssim 1$) one has $K_{2\tau} \gg 1$ and for the muon-dominated solutions ($K_{1\mu}$) one has $K_{2\tau_2^\perp} \gg 1$ (except for very few points with $K_{2\tau_2^\perp} \simeq 1$). As we will discuss, there are also some electron dominated solutions that entirely depend on the initial N_2 abundance, since $K_{2\tau_2^\perp} \lesssim 1$, but for low $\tan \beta$ values they are marginal and do not influence the constraints on the low energy neutrino parameters. They correspond to the sparse point at $K_{1\tau} \gg 1$ and in the range $1 \text{ meV} \lesssim m_1 \lesssim 10 \text{ meV}$. The low density indicates that these solutions are marginal and require some fine tuning to realise weak wash-out at the production, i.e. $K_{2\tau_2^\perp} \lesssim 1$, and to enhance the CP asymmetry $\varepsilon_{2\alpha}$.

Coming back to the leading tauon dominated solutions, notice that in principle since the washout is stronger compared to the SM case, because of the smaller value of m_\star^{MSSM} compared to m_\star^{SM} (cf. eq. (12)), one could think that it should be more difficult to realise the condition $K_{1\tau} \lesssim 1$. However, from the analytical expression given in [18] for $V_L = I$, extended to the supersymmetric case with the simple replacement $m_\star^{SM} \rightarrow m_\star^{MSSM}$, explicitly

$$K_{1\tau} \simeq \frac{|c_{13} c_{12} s_{12} s_{23} (m_1 e^{2i\rho} - m_2) + s_{13} c_{13} c_{23} (m_3 e^{i(2\sigma-\delta)} - m_2 s_{12}^2 e^{i\delta} - m_1 c_{12}^2 e^{i(2\rho+\delta)})|^2}{m_\star^{MSSM} |m_1 c_{12}^2 c_{13}^2 e^{2i\rho} + m_2 s_{12}^2 c_{13}^2 + m_3 s_{13}^2 e^{2i(\sigma-\delta)}|}, \quad (30)$$

one can see that the slightly lower value of m_\star^{MSSM} plays just a marginal role since the condition $K_{1\tau} \lesssim 1$ produces conditions on the phases marginally dependent on m_\star^{MSSM} . Actually the increase of the asymmetry of a factor $\sim \sqrt{2}$ at the production, due to the doubled CP asymmetry only partly compensated by a stronger wash-out, enlarges the allowed region in the plane θ_{23} vs. m_1 at values $m_1 \simeq 50 \text{ meV}$, the so called τ_B solution and, more generally, the allowed range of m_1 gets slightly wider (for example the upper bound relaxes from 0.06 eV to 0.1 eV).

The blue points in Fig. 1 are the subset satisfying the strong thermal condition (dark blue for $I \leq V_L \leq V_{CKM}$, light blue for $V_L = I$) for an initial pre-existing asymmetry $N_{B-L}^{\text{p,i}} = 10^{-3}$. Also in this case we can compare the results with the non-supersymmetric case. This time there is one significant difference since in the supersymmetric case the strong thermal region is more extended and in particular it allows higher values of the atmospheric mixing angle. Indeed while in the non-supersymmetric case one has a quite stringent upper bound on the atmospheric mixing angle $\theta_{23} \lesssim 43^\circ$, in the supersymmetric case this now gets relaxed to $\theta_{23} \lesssim 46^\circ$, a relaxation that might be relevant in view of the

next expected results from long baseline experiments.

This relaxation is quite well explained analytically for $V_L = I$ extending to the supersymmetric case the discussion in [18]. The upper bound on θ_{23} indeed originates from the requirement $K_{1e} \gg 1$ from the strong thermal condition. This condition first translates into a lower bound on the $0\nu\beta\beta$ effective neutrino mass $m_{ee} \gtrsim 8 \text{ meV}$ and then into one on the lightest neutrino mass $m_1 \gtrsim 1.3 m_{ee} \gtrsim 10 \text{ meV}$ [22]. Since in the supersymmetric case all $K_{i\alpha}$ are $\sim \sqrt{2}$ larger, this requirement is now more easily satisfied and one has $m_{ee} \gtrsim 6 \text{ meV}$ giving $m_1 \gtrsim 7 \text{ meV}$, well explaining the constraints in the plane m_{ee} vs. m_1 (see bottom left panel in Fig. 1), and this in turn implies indeed $\theta_{23} \lesssim 46^\circ$.

In Fig. 2 we show 6 panels, for integer values of α_2 from one to six, of the RH neutrino masses M_i and of the minimum requested value of T_{RH} (we will discuss this in detail separately in Section 4). In these panels we have highlighted the flavour that dominates the asymmetry associating a different colour to each flavour (blue for tauon, green for muon, red for electron). The points are calculated in the case $I \leq V_L \leq V_{CKM}$ and again for initial thermal N_2 abundance. As one can see, in addition to muon (green points) and tauon (blue points) flavour dominated solutions, also electron flavour dominated solutions are present. At low α_2 values ($\alpha_2 = 1, 2$) these are even the only solutions for $m_1 \lesssim 20 \text{ meV}$. For $V_L = I$ the electron flavour asymmetries are many order of magnitude suppressed compared to the muonic and even more compared to the tauonic [18] but when $V_L \neq I$ this sharp flavour dominance does not hold [17]. In the non-supersymmetric case we have also found electron-flavour dominated solutions but in a very marginal way. This means that these solutions realise successful leptogenesis only for very special conditions in the non-supersymmetric case and the maximum possible asymmetry is just very slightly above the observed value. In the supersymmetric case, since the CP asymmetries double and the wash-out at the production is only $\sim \sqrt{2}$ stronger, the $B - L$ asymmetry at the production is $\sim \sqrt{2}$ higher and this helps the marginal electron-dominated solutions to be realised for a slightly wider region in parameter space in any case without really opening up new allowed regions in the low energy neutrino parameters. At the same time it is important to stress that since these solutions are realised for $K_{2\tau_2^\perp} \lesssim 1$, they are strongly dependent on the initial N_2 abundance and, in particular, they completely disappear for initial vanishing N_2 abundance.

In conclusion for low $\tan \beta$ values the low energy neutrino constraints are only slightly more relaxed than in the non-supersymmetric case and in particular, as we have seen, the strong thermal condition is satisfied for slightly lower m_1 values.

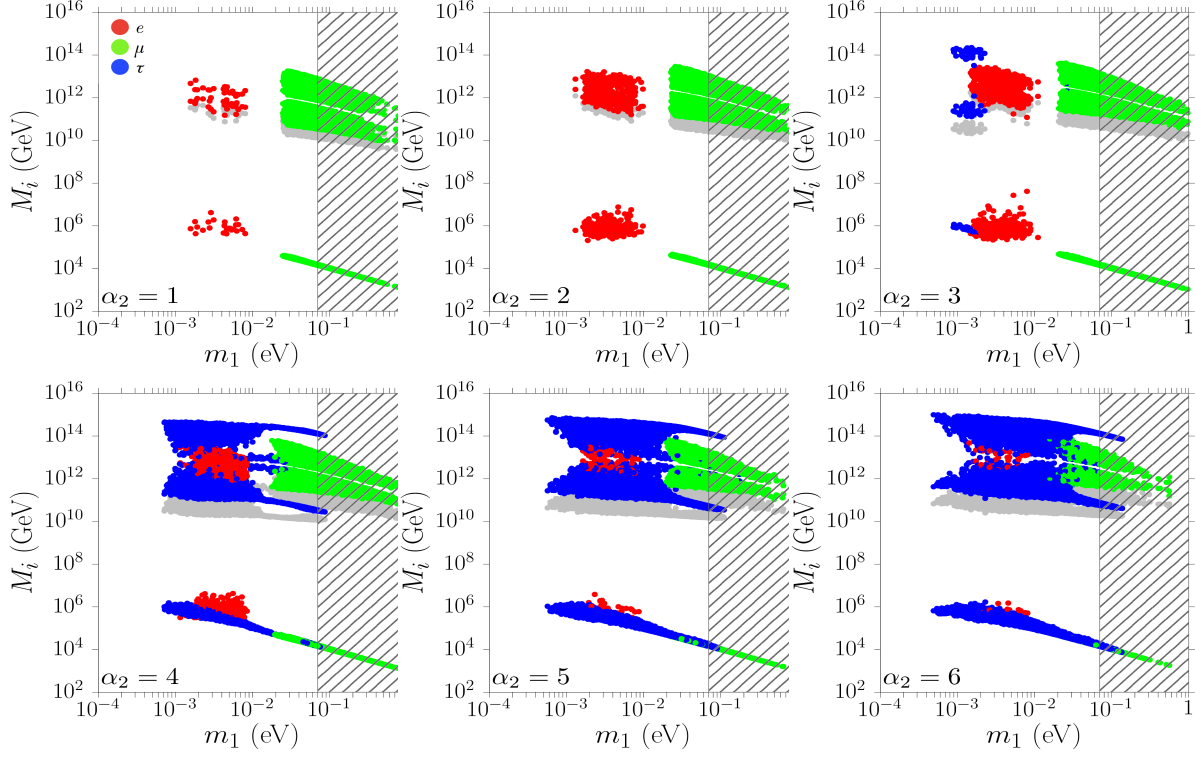


Figure 2: Scatter plots in the low energy neutrino parameter space projected on the plane M_i vs. m_1 for NO, $\tan \beta = 5$ and for integer $\alpha_2 = [1, 6]$ from top left to bottom right. All points respect the successful leptogenesis condition $\eta_B^{\text{lep}} > \eta_B^{\text{CMB}} > 5.9 \times 10^{-10}$ for $I \leq V_L \leq V_{\text{CKM}}$. The dashed region indicate the value of m_1 excluded by the *Planck* upper bound eq. (27). The red, green and blue points are those for which the final asymmetry is dominated by the electron, muon and tauon flavour respectively. The grey points indicate the minimum value of T_{RH} .

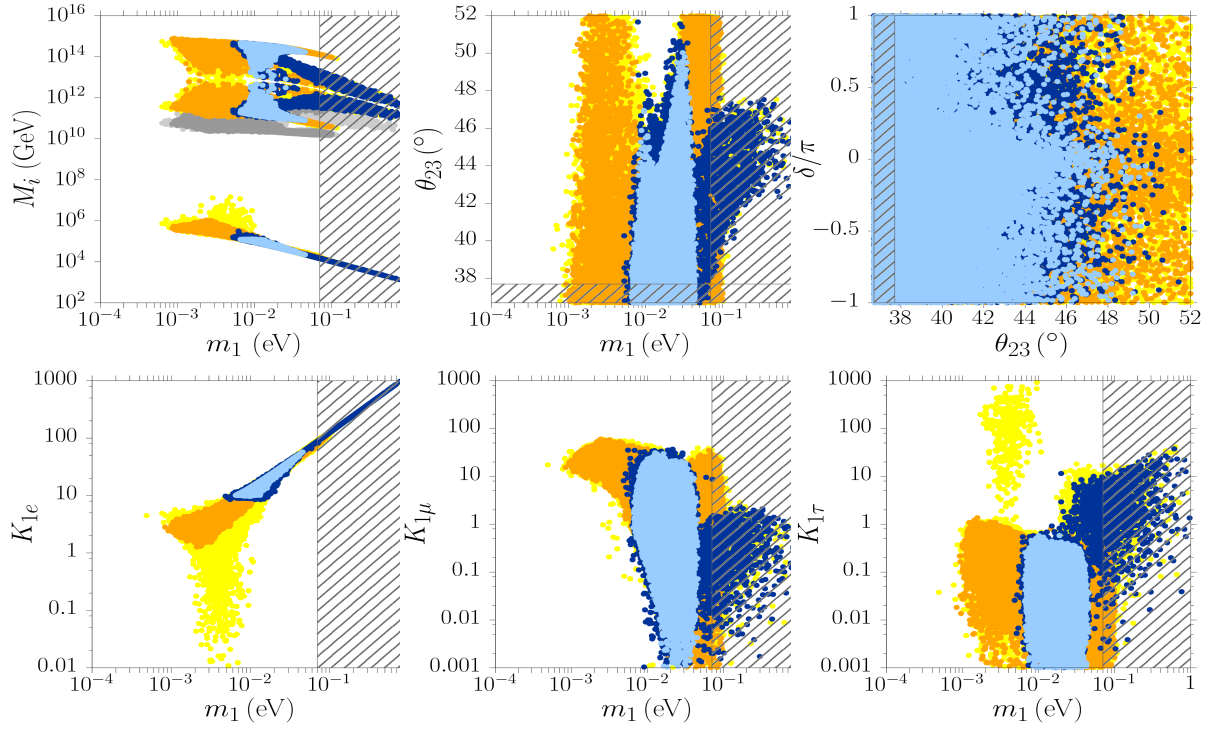


Figure 3: Same scatter plots as in Fig. 1 but for $\tan \beta = 50$.

3.1.2 Large $\tan \beta$ values ($\tan \beta = 50$)

Let us see now what happens when $\tan \beta$ is large enough that the production occurs in the three-flavoured regime. There is no explicit dependence of the asymmetry on $\tan \beta$, the dependence is all encoded in the values of M_2 marking the transitions between two different flavoured regimes. The results will be the same for all $\tan \beta$ values large enough to lead to a production in the three flavoured regime for all allowed values of M_2 . Since the condition for the three-flavoured regime is $M_2 \lesssim 5 \times 10^8 \text{ GeV} (1 + \tan^2 \beta)$ and since one expects $M_2 \gtrsim 10^{10} \text{ GeV}$, some solutions occurring in the three-flavoured regime are expected to appear for $\tan \beta \gtrsim 5$. On the other hand since there are no solutions for $M_2 \gtrsim 3 \times 10^{12} \text{ GeV}$, for $\tan \beta \gtrsim 80$ all solutions fall in the three flavoured regime. We choose for definiteness $\tan \beta = 50$. This is sufficiently large that basically all solutions fall in the three flavoured regime so that constraints on low energy neutrino data are saturated increasing $\tan \beta$. The results are shown in Fig. 3. The panels, the colour codes and all benchmark values are the same as in Fig. 1, so that there can be a straightforward comparison with the results obtained for $\tan \beta = 5$. Looking at the yellow (and orange) points, those satisfying only the successful leptogenesis condition, one can notice that the constraints are even more relaxed than in the previous case for $\tan \beta = 5$ compared to the non-supersymmetric case. There is still a lower bound on the lightest neutrino mass

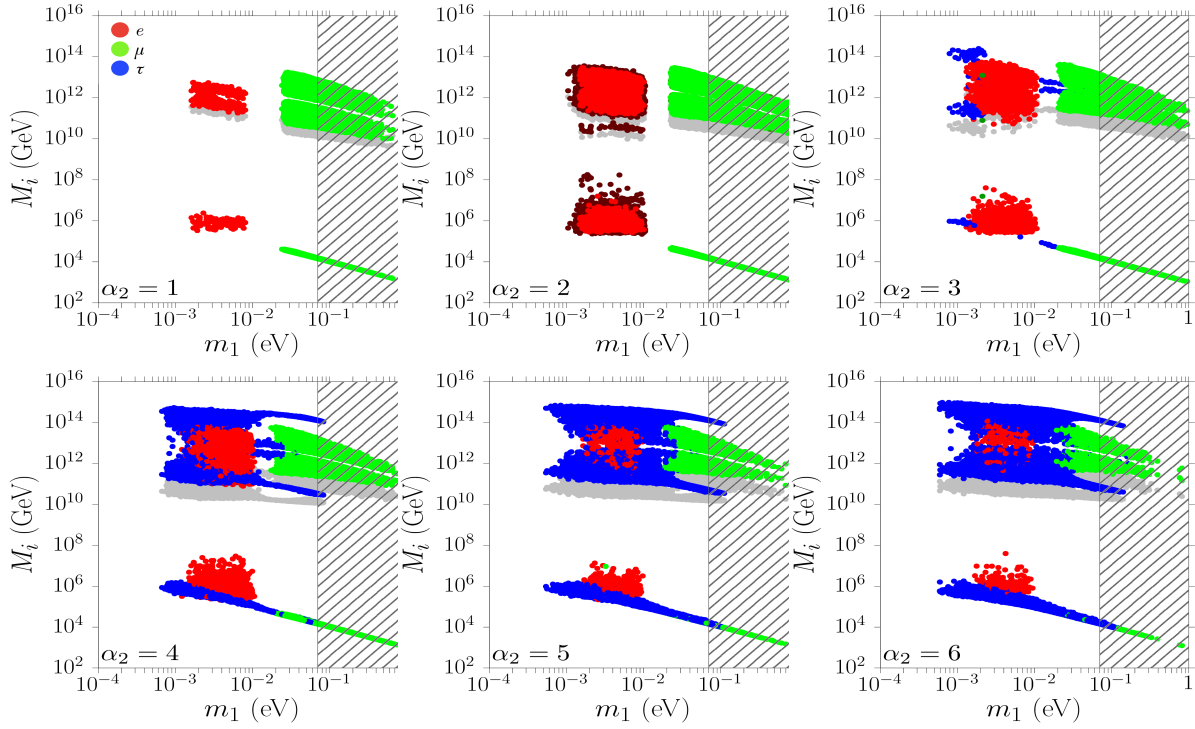


Figure 4: Scatter plots as in Fig. 2 but for $\tan \beta = 50$. In the top central panel for $\alpha_2 = 2$, the dark (light) red points are solutions for $|\Omega_{ij}|^2 > 3$ ($|\Omega_{ij}|^2 < 3$) able to lower T_{RH} below 10^{10} GeV.

$m_1 \gtrsim 1$ meV that is just very slightly relaxed compared to non-supersymmetric case (the CP asymmetry doubles but the value of $K_{2\tau}$ determining the wash-out at the production gets $\sim \sqrt{2}$ higher and the two effects almost cancel out). This is interesting because one can conclude that the lower bound on m_1 is quite a stable and general feature of $SO(10)$ -inspired models that, therefore, predict some deviation from the hierarchical limit though this might well be below current experimental sensitivity. Indeed in the most optimistic case cosmological observations should place a 2σ upper bound $m_1 \lesssim 10$ meV [51, 52].

From Fig. 3 it should be also noticed how the region satisfying $K_{1e} \lesssim 1$ now greatly enlarges compared to the large $\tan\beta$ case. Indeed, if one looks at the panels in Fig. 4, showing again (as in Fig. 2 but now for $\tan\beta = 50$) what flavour dominates the final asymmetry, one can notice how this time there are plenty of electron dominated solutions, in the range for $2 \text{ meV} \lesssim m_1 \lesssim 10 \text{ meV}$, as anticipated. This region was very marginal, almost absent, in the non-supersymmetric case and it was still quite marginal also for $\tan\beta = 5$, as discussed. However now, for $\tan\beta = 50$, it becomes quite significant and as we will discuss in the next section, it allows a relaxation of the lower bound on T_{RH} below 10^{10} GeV for $1 \lesssim \alpha_2 \lesssim 2$. We should however stress again that these electron dominated solutions occur in the weak wash-out regime at the production ($K_{2e} \lesssim 1$) and, therefore, they strongly depend on the initial N_2 abundance. They exist for initial thermal N_2 abundance but for vanishing initial N_2 abundance they completely disappear (i.e. they do not realise successful leptogenesis). The reason why they are obtained much easier at large $\tan\beta$ values compared to low $\tan\beta$ values is because now the condition of weak wash-out at the production is more relaxed, $K_{2e} \lesssim 1$ instead of $K_{2\tau_2^\perp} \equiv K_{2e} + K_{2\mu} \lesssim 1$.

If we again consider the subset of points satisfying also the strong thermal condition (dark and light blue points), we can see that, as in the low $\tan\beta$ case, the region is now much more extended, even more than before. This happens because of the effect explained at the end of Section 2: one can now have $K_{1\mu} \lesssim 1$ and at the same time wash-out the pre-existing asymmetry in all flavours imposing $K_{1e}, K_{2\mu}, K_{2\tau} \gg 1$. This opens up a new (muon dominated) region at large values of $m_1 \gtrsim 0.05$ eV, though notice that this is now largely excluded by the upper bound Eq. (27).

3.2 Inverted ordering

Let us now discuss the IO case distinguishing, as we did for NO, small $\tan\beta$ values ($\lesssim 15$) from large $\tan\beta$ values ($\gtrsim 15$).

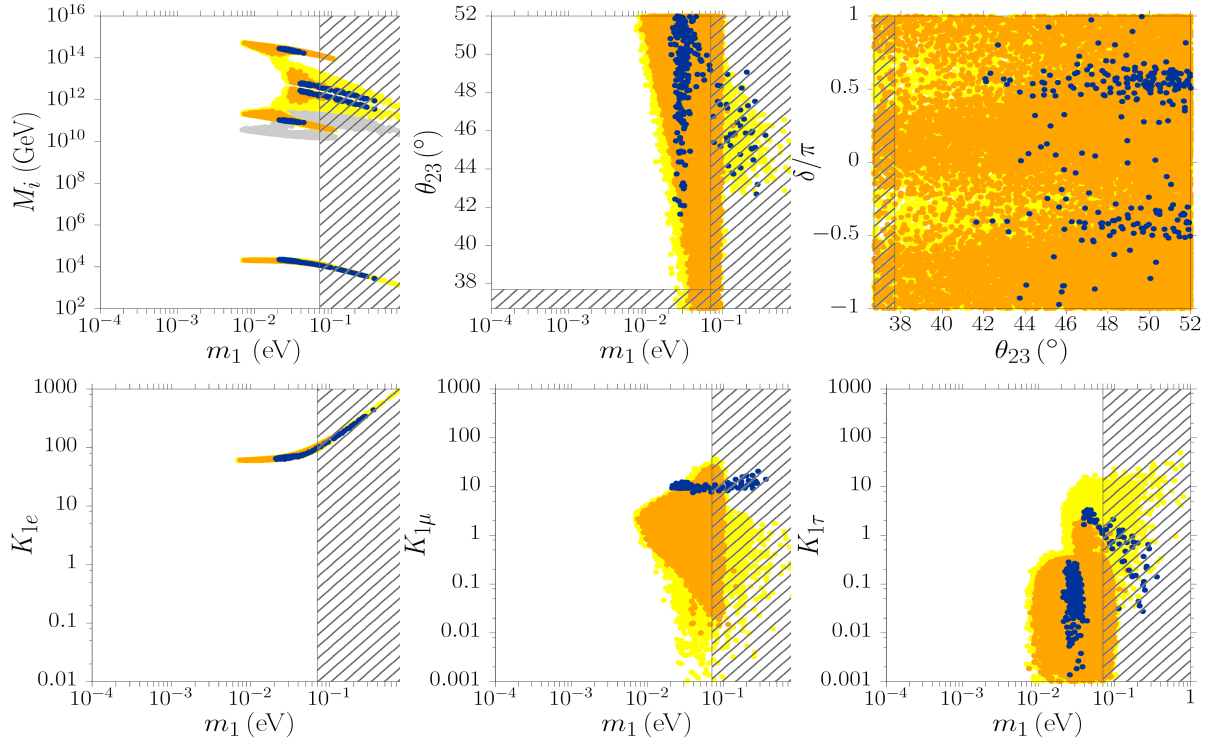


Figure 5: Scatter plots as in Fig. 1 but for IO and $\tan \beta = 5$.

3.2.1 Small $\tan \beta$ values

For small $\tan \beta$ values the situation is, as for NO, similar to the non-supersymmetric case though the allowed regions are slightly more relaxed. In Fig. 5 we show the results again for $\tan \beta = 5$ and one can see in particular that:

- there is a lower bound $m_1 \gtrsim 10 \text{ meV}$ corresponding to $\sum m_i \gtrsim 130 \text{ meV}$ that will be in a close future tested by the cosmological observations;
- this time, differently from the non-supersymmetric case, there is no lower bound on the atmospheric mixing angle, though values in the first octant require higher values of the absolute neutrino mass scale on the verge of being excluded by the cosmological observations.

We can therefore conclude again, as in the non-supersymmetric case, that the IO case is disfavoured compared to the NO case.

In Fig. 6 we show again, with the same colour code as in Fig. 2 and 4 for NO, the solutions for various values of α_2 indicating the flavour that dominates the final asymmetry. This time one can see that, even for initial thermal N_2 -abundance, there are no electron dominated solutions. The reason is simply that in the IO case one has $K_{1e} =$

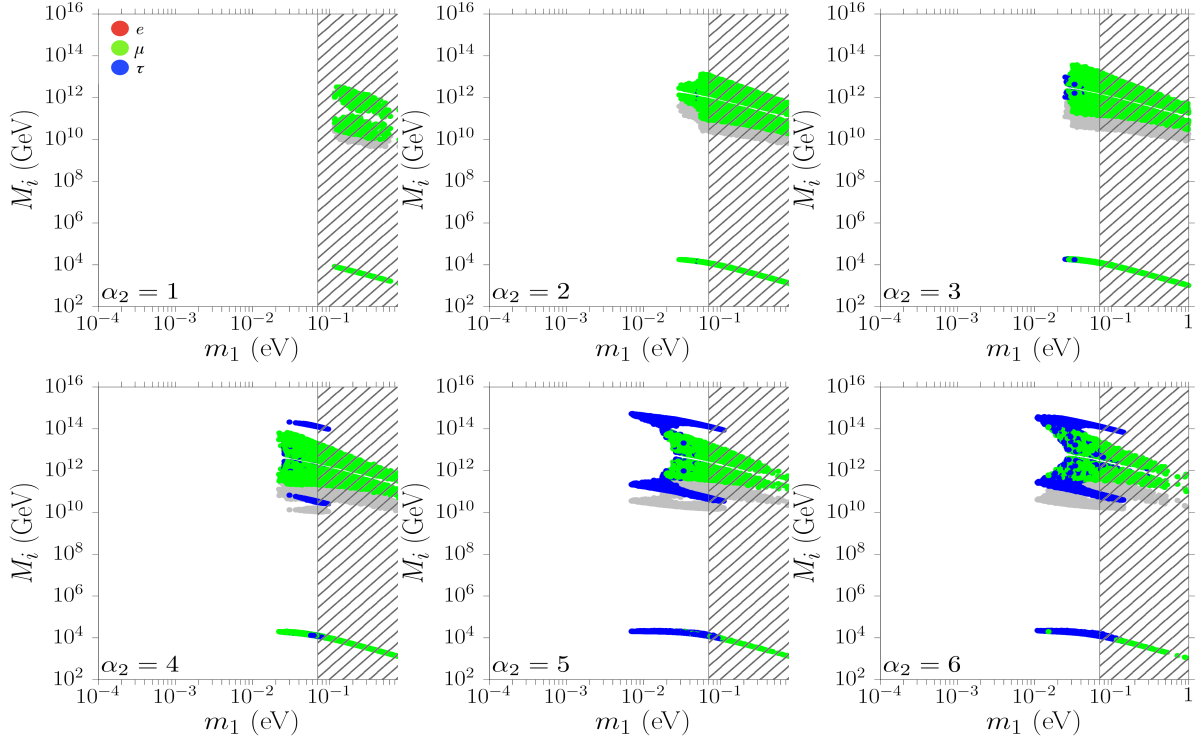


Figure 6: Scatter plots as in Fig. 2 but for IO and $\tan \beta = 5$.

$m_{ee}/m_\star^{MSSM} \gtrsim 70$ [18] and, therefore, the electron asymmetry is completely washed-out by the lightest RH neutrinos inverse processes.

3.2.2 Large $\tan \beta$ values

For large $\tan \beta$ values and imposing successful leptogenesis condition, the situation is qualitatively similar to the case of small $\tan \beta$ as one can see from Fig. 7 (orange and yellow points) but simply the allowed regions slightly further enlarge. For example now one has $m_1 \gtrsim 7$ meV. In the panels of Fig. 8 we show the dominant flavour and one can see that, for the same reason, there are no electron dominated solutions (no red points). The real difference is that now there is a large amount of solutions satisfying the strong thermal leptogenesis condition. The reason is that for large $\tan \beta$ the fact that $K_{1\mu}$ tends not to be too large (see central bottom panel in Fig. 7), is not a problem, since the condition for the wash-out of the pre-existing asymmetry now requires $K_{1\mu} + K_{2\mu} \gg 1$ and it can be more easily satisfied even for low $K_{1\mu}$ values. We can conclude that in all cases supersymmetry helps realising the strong thermal condition.

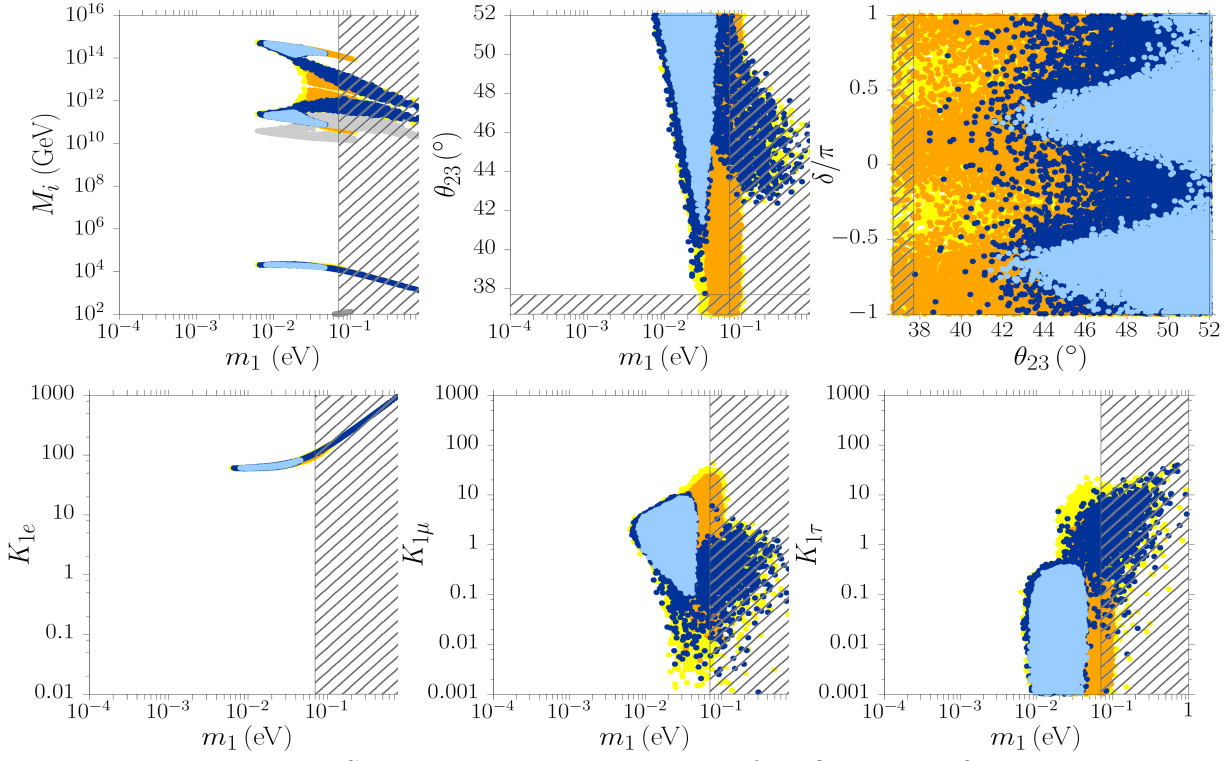


Figure 7: Scatter plots as in Fig. 1 but for IO and $\tan \beta = 50$.

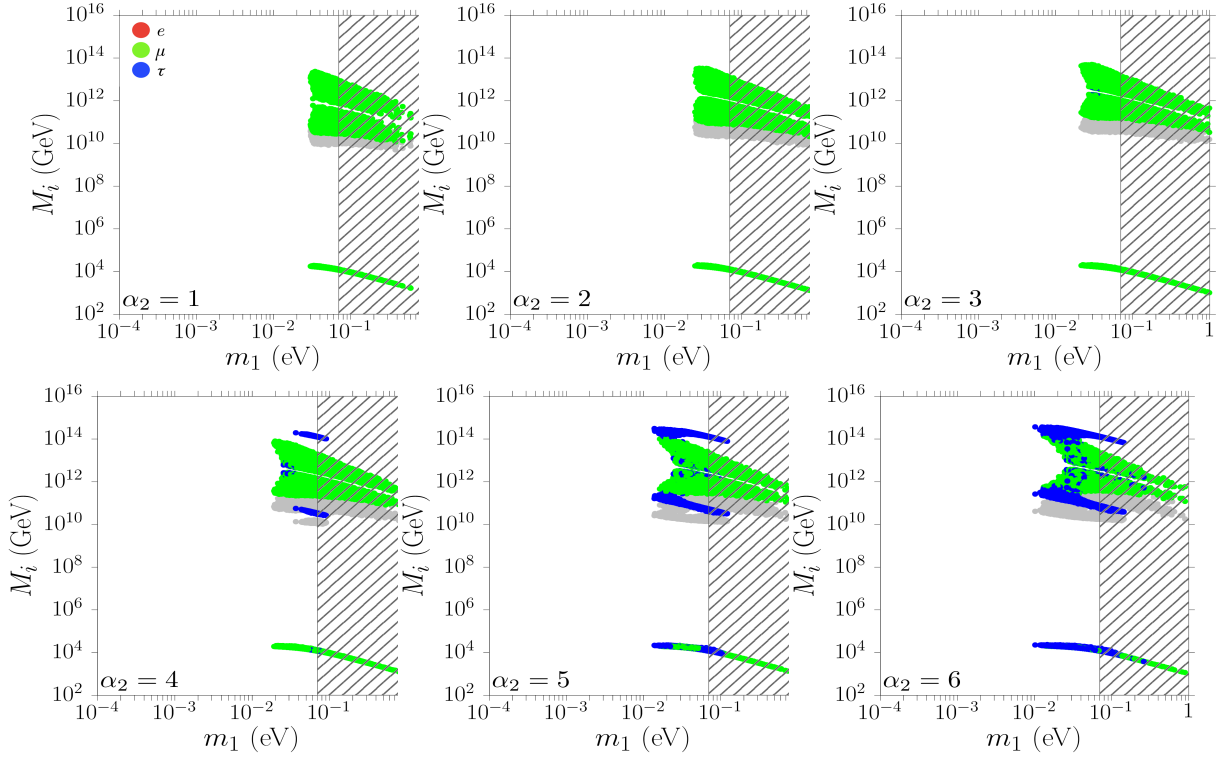


Figure 8: Scatter plots as in Fig. 2 but for IO and $\tan \beta = 50$.

4 Lower bound on T_{RH}

Thermal leptogenesis requires the initial temperature of the radiation dominated regime, T_{RH} within inflation, to be sufficiently high for the RH neutrinos to be thermally produced before their interactions with the thermal bath, in particular their inverse decays, go out-of-equilibrium.

For a specific solution this occurs at a temperature $T_{\text{lep}}(K_{2\alpha}) \simeq M_2/z_B(K_{2\alpha})$, where α is the flavour in equilibrium that dominates the asymmetry, either τ or τ_2^\perp in the two fully flavoured regime, or $\alpha = e, \mu$ or τ in the three fully flavoured regime.¹⁰

At higher temperatures, in the strong wash-out regime ($K_{2\alpha} \gg 1$), the produced asymmetry is efficiently washed-out, while at lower temperatures, since the RH neutrino abundance is dropping exponentially, the produced asymmetry is negligible. In this way the asymmetry, in each flavour in equilibrium, is produced within quite a well defined range of temperatures between $M_2/[z_B(K_{2\alpha}) - 2]$ and $M_2/[z_B(K_{2\alpha}) + 2]$ [20]. Therefore, for a specific solution the reheat temperature has to be greater than $T_{\text{RH}}^{\text{min}}(K_{2\alpha}) \simeq M_2/[z_B(K_{2\alpha}) - 2]$. In the weak wash-out regime one cannot identify such a sharp interval of temperatures and moreover the process of production of the asymmetry depends on the initial N_2 abundance. In this case one can say that $T_{\text{RH}} \gtrsim M_2$ for the final asymmetry to be equal to the asymptotic value at high temperatures. An expression that interpolates quite well $T_{\text{RH}}^{\text{min}}(K_{2\alpha})$ between the strong and weak wash-out regime is given then by [20]

$$T_{\text{RH}}^{\text{min}}(K_{2\alpha}) \simeq \frac{M_2}{z_B(K_{2\alpha}) - 2 e^{-\frac{3}{K_{2\alpha}}}}. \quad (31)$$

This expression gives, for each solution with specified values of $K_{2\alpha}$ and M_2 , the minimum T_{RH} . The lower bound on T_{RH} can then be calculated minimising over all the found solutions, i.e. $T_{\text{RH}}^{\text{min}} \equiv \min[T_{\text{RH}}^{\text{min}}(K_{2\alpha})]$.

In the non-supersymmetric case it was obtained $T_{\text{RH}}^{\text{min}} \simeq 1 \times 10^{10}$ GeV for $\alpha_2 = 1$ [17], a lower bound that cannot be excluded by any experimental observation or theoretical argument. However, this result could somehow suggest that also in the supersymmetric case one can expect a similar or even more stringent lower bound because of the increased wash-out, leading in this case to a tension with the gravitino problem upper bound that, as discussed in the introduction, in a conservative way can be assumed to be $T_{\text{RH}} \lesssim 10^{10}$ GeV in order not to overproduce the gravitino abundance.¹¹

¹⁰Of course there could be a fine tuned situation where the contributions from different flavours are equivalent, in this case one should have T_{RH} above the maximum value out of the three $T_{\text{RH}}^{\text{min}}(K_{2\alpha})$.

¹¹The exact value depends on the neutralino mass and in particular is inversely proportional to it, values as large as $T_{\text{RH}} \simeq 2 \times 10^{10}$ GeV are acceptable [31].

This potential tension was confirmed by a dedicated analysis made in the supersymmetric case [35]. Here it was obtained (for $\alpha_2 = 5$) $T_{\text{RH}} \gtrsim 10^{11}$ GeV, a result that would suggest that $SO(10)$ -inspired thermal leptogenesis is incompatible with the upper bound from the gravitino problem unless, as discussed in the introduction, one assumes very specific supersymmetric models.

We plotted $T_{\text{RH}}^{\text{min}}(K_{2\alpha})$ for each point satisfying successful leptogenesis. The values of $T_{\text{RH}}^{\text{min}}(K_{2\alpha})$ are shown with grey points in all plots where also the RH neutrino masses are plotted. These plots are shown in Figs. 2, 4, 6, 8 for NO low $\tan\beta$, NO high $\tan\beta$, IO low $\tan\beta$ and IO high $\tan\beta$ respectively for six specific integer values of α_2 (from 1 to 6) since one can expect a non trivial dependence on α_2 . This is because for decreasing α_2 one has that M_2 decreases and this would go into the direction to lower T_{RH} . On the other hand the final asymmetry decreases as $\propto \alpha_2^2$ so that there is also a lower bound on α_2 coming from successful leptogenesis. In these figures one can see indeed how the allowed range of values for $T_{\text{RH}}^{\text{min}}(K_{2\alpha})$ depends on α_2 .

Finally, in Fig. 9 we summarised the results plotting the lower bound $T_{\text{RH}}^{\text{min}}$ as a function of α_2 indicating, with the same colour code as in Figures 2, 4, 6 and 8, which flavour dominates the asymmetry for each value of α_2 . The results are shown both for initial thermal N_2 abundance (thin lines) and for vanishing initial N_2 abundance (thick lines). The main difference is that in the second case there are no electron-dominated solutions since these all have weak wash-out at the production ($K_{2e} \lesssim 1$) and the asymmetry is strongly suppressed in the case of initial N_2 vanishing abundance. In the left (right) panels we show the results for low (high) values of $\tan\beta$, in the top (bottom) panels the results for NO (IO). In the case of low $\tan\beta$ values (left panels) one can see how the results do not actually differ that much from those in the non-supersymmetric case [17]. There is actually even a $\sim \sqrt{2}$ relaxation due to the fact that the asymmetry increases by a factor ~ 2 because of the doubled CP asymmetry and the efficiency factor decreases of a factor $\sim \sqrt{2}$ (the efficiency factor is approximately inversely proportional to the decay parameters that increase of a factor $\sqrt{2}$).

However, in the right panels, for large $\tan\beta$ values, one can see how the red branch, corresponding to the electron flavour dominated solutions now, for $\alpha_2 = 1-2$, allows $T_{\text{RH}}^{\text{min}} \simeq (5-10) \times 10^9$ GeV, showing that it is possible to go even below 10^{10} GeV. Notice however that these electron-flavour dominated solutions have two drawbacks. First they exist only for initial thermal N_2 abundance, a case that should be justified within models where for example the RH neutrinos are produced by Z' particles, heavier than the N_2 's, of a left-right symmetry after $SO(10)$ breaking [53]. Moreover those solutions minimising $T_{\text{RH}}^{\text{min}}$ below 10^{10} GeV are characterised by large values of the squared modules of the

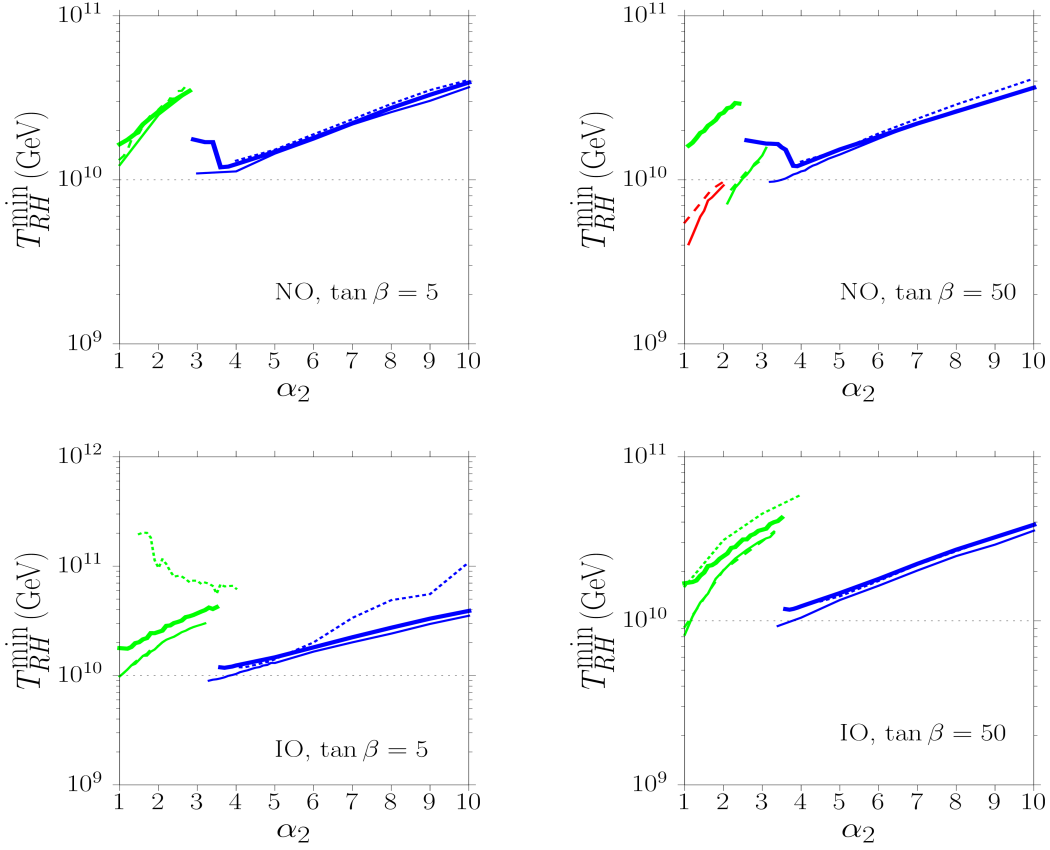


Figure 9: Lower bound on T_{RH} as a function of α_2 . The blue, green and red lines correspond to an asymmetry tauon, muon and electron dominated respectively. The thin lines are for initial thermal N_2 abundance. The solid lines are for $I \leq V_L \leq V_{CKM}$, the dashed lines for $V_L = V_{CKM}$, the dotted lines for $V_L = I$. The thick solid lines are for initial vanishing abundance and $I \leq V_L \leq V_{CKM}$. The top (bottom) panels are for NO (IO). The left (right) panels are for $\tan \beta = 5$ (50).

orthogonal matrix entries (implying strongly fine tuned cancellations in the see-saw formula). This happens because the N_2 CP asymmetries are not upper bounded and they are enhanced when $|\Omega_{ij}|^2 \gg 1$. In the $\alpha_2 = 2$ panel of Fig. 4 (bottom central panel) these fine tuned solutions correspond to the dark red points. One can see how they also correspond to uplifted values of M_1 and reduced values of M_2 (they are indeed in the vicinity of crossing level solution).

For these reasons these solutions should not be over emphasized, though they still represent a possibility that should not be disregarded. On the other hand the muon and the tauon-flavour dominated solutions, that give $T_{\text{RH}}^{\text{min}} \sim 10^{10}$ GeV, are not fine tuned and correspond to typical $SO(10)$ -inspired solutions. Moreover in the case of the tauon dominated solutions they are also genuinely strong washed solutions independent of the initial N_2 abundance.

Notice that the lower bound on T_{RH} that we found for $\alpha_2 = 5$, $T_{\text{RH}} \gtrsim 1.5 \times 10^{10}$ GeV, is more than one order of magnitude below the lower bound found in [35]. We cannot explain the origin of the discrepancy since details of the calculation of the final asymmetry (for example how the matrix U_R is calculated) are not specified in [35]. We can only report that in [35] the tauon-dominated solutions that we find are absent and the result on the T_{RH} lower bound mainly relies on the electron dominated solutions and therefore on the assumption of initial thermal N_2 abundance.

Our result for the lower bound on the reheat temperature, $T_{\text{RH}}^{\text{min}} \gtrsim 1 \times 10^{10}$ GeV, is approximately equal to the value that one needs in order to produce the Dark Matter gravitino abundance depending on the value of the gluino masses. This coincidence is similar to what happens in the case of traditional N_1 -dominated leptogenesis [54] so that one could intriguingly relate matter-antimatter asymmetry production in thermal leptogenesis to gravitino Dark Matter production. On the other hand the recent LHC results on the lower bound of gluino masses [2] make the upper bound on T_{RH} more stringent, at the level of $T_{\text{RH}} \lesssim 5 \times 10^9$ GeV within the pMSSM [55] and this seems to corner this intriguing scenario of thermal leptogenesis combined with gravitino Dark Matter. However, as already mentioned, for large values of the gravitino mass ($\gtrsim 30$ TeV) the large T_{RH} required by SUSY $SO(10)$ -inspired thermal leptogenesis ($T_{\text{RH}} \gtrsim 10^{10}$ GeV) can be reconciled with the gravitino problem. Of course within specific realistic models one should verify whether the lower bound $T_{\text{RH}}^{\text{min}} \sim 10^{10}$ GeV can be indeed saturated.

There is, however, still another possibility, never considered so far, that can allow a relaxation of $T_{\text{RH}}^{\text{min}}$ even below 10^{10} GeV for usual tauon-flavour solutions.

5 A new scenario of N_2 -dominated leptogenesis

It is usually assumed that the lightest RH neutrino mass $M_1 \gtrsim T_{\text{sph}}^{\text{out}} \simeq 100 \text{ GeV}$, where $T_{\text{sph}}^{\text{out}}$ is the sphaleron freeze-out temperature [56]. In this case the lightest RH neutrino wash-out has to be taken into account. However, if M_1 is below such a temperature, then the lightest RH neutrino wash-out acts only on the lepton asymmetry but not on the frozen baryon asymmetry produced earlier by N_2 out-of-equilibrium decays.¹² In this case the final asymmetry is given by the expressions eqs. (8), (9), (10) without the exponentials encoding the lightest RH neutrino wash-out since this is negligible.

We have then repeated the calculation of $T_{\text{RH}}^{\text{min}}$ in this scenario and the results are shown in the four panels of Fig. 10 that correspond to the same cases of the panels in Fig. 9. This time the minimum is always realised by tauon dominated solutions with strong wash-out at the production where the final asymmetry is independent of the initial N_2 abundance. It can be seen how values of T_{RH} as low as 10^9 GeV are possible. In this case the gravitino overabundance problem can be circumvented for a wider range of gravitino masses compared to the traditional scenario discussed in the previous sections.

From the expression eq. (7) for M_1 one can see how this scenario requires values $\alpha_1 \lesssim 0.1$ (for hierarchical neutrinos, if $m_1 \gtrsim 10 \text{ meV}$ one can have higher values). This would also imply somehow that also $m_{D3} \ll T_{\text{sph}}^{\text{out}} \sim 100 \text{ GeV}$ in order for the seesaw formula to be valid implying $\alpha_3 \ll 1$. One can wonder whether this can be achieved in some realistic models. Interestingly in a recent study of realistic $SO(10)$ models [28] one of the found best fit cases, a supersymmetric model with $10_H, 120_H, 1\bar{26}_H$ Higgs representations, is realised for $M_1 \simeq 1 \text{ TeV}$ corresponding to $\alpha_1 \simeq 0.3$. Since this case also has a very small $\chi_{\text{min}}^2 \simeq 0.6$, one can wonder whether with some deviation from the best fit one could get $M_1 \lesssim T_{\text{RH}}^{\text{sph}}$ with still an acceptable value of χ_{min}^2 . In any case this specific example seems to suggest that this scenario might be indeed realised within some realistic model. Notice that within this scenario we are not showing the low energy neutrino constraints since these simply evaporate. Indeed these constraints exist mainly because of the presence of the lightest RH neutrino wash-out, as stressed in previous papers [16, 17, 18]. It should also be made clear that though we are presenting this scenario in a supersymmetric framework, where it nicely allows T_{RH} values below 10^{10} GeV , it might be also realised and find applications within a non-supersymmetric framework.

¹²More precisely the N_1 wash-out acts in an interval of temperatures $T = [M_1/z_{\text{in}}, M_1/z_{\text{out}}]$ with $z_{\text{in}} \simeq 2/\sqrt{K_{1\alpha}}$ [20]. Therefore, more precisely one has to impose $M_1 \lesssim z_{\text{in}} T_{\text{sph}}^{\text{out}}$.

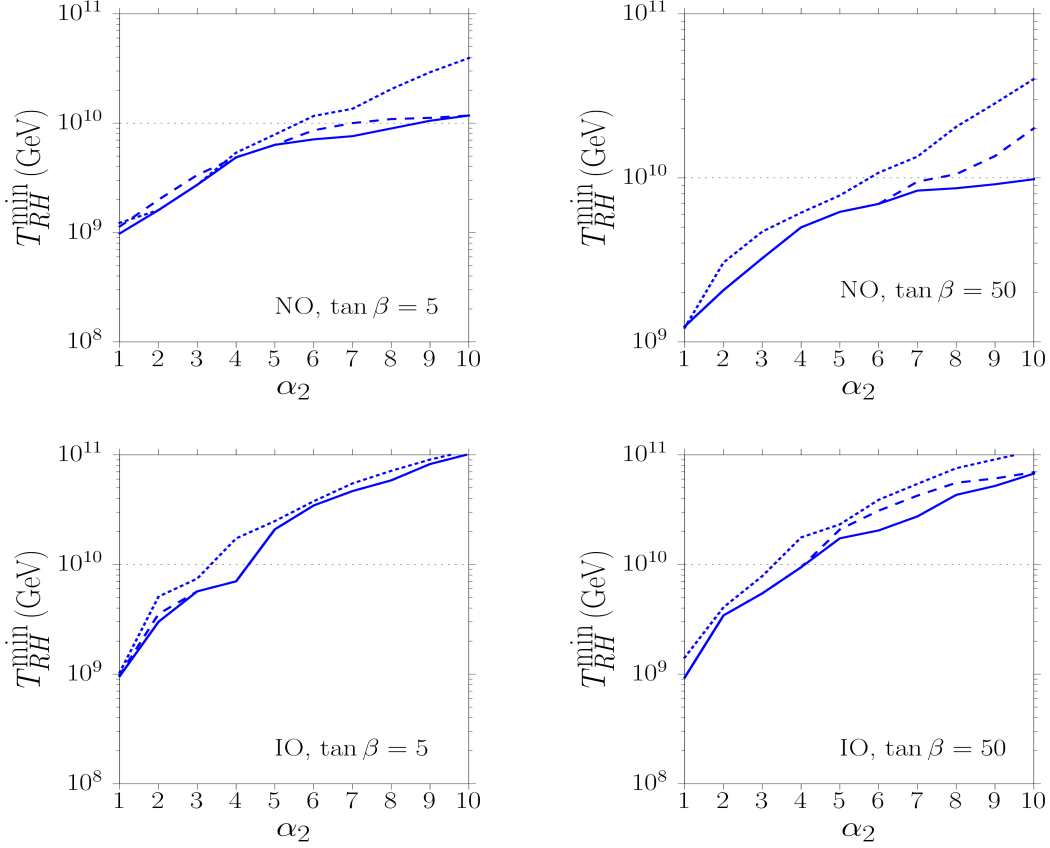


Figure 10: Lower bound on T_{RH} as a function of α_2 in a scenario where $M_1 \lesssim T_{\text{sph}}^{\text{out}} \simeq 100 \text{ GeV}$. The left (right) panels are for $\tan \beta = 5(50)$, the top (bottom) panels are for NO (IO). Same line conventions as in Fig. 9 with the difference that this time there is no distinction between thin and solid lines since there is no dependence on the initial N_2 abundance.

6 Conclusions

We extended the study of $SO(10)$ -inspired leptogenesis, previously discussed in a non-supersymmetric framework, to the supersymmetric case calculating the constraints on the low energy neutrino parameters and the lower bound on T_{RH} that has a particular importance because of the tension with the upper bound from the gravitino problem. Our results show that, in the usual case, where the lightest RH neutrino mass is heavier than the sphaleron freeze-out temperature and N_1 wash-out is present, values of T_{RH} as low as $T_{\text{RH}} \simeq 1 \times 10^{10} \text{ GeV}$ are possible without any fine-tuning and for a final asymmetry independent of the initial N_2 -abundance. We have then proposed a novel scenario where M_1 is below the sphaleron freeze-out temperature so that the N_1 wash-out is absent. In this case without any fine-tuning reheat temperature values as low as $T_{\text{RH}} \simeq 1 \times 10^9 \text{ GeV}$ are allowed. In our calculation the main neglected effects that could produce some significant modifications are flavour coupling effects [26] arising from a redistribution of the asymmetry among quarks, right handed charged leptons and above all Higgs (and of course also among the supersymmetric particles [41]). This could open new way to circumvent the N_1 wash-out but in any case it should be clear that an account of these effect can at most relax the reheat temperature in the scenario where $M_1 \gtrsim T_{\text{sph}}^{\text{out}}$ to the minimum value, $T_{\text{RH}}^{\text{min}} \simeq 1 \times 10^9 \text{ GeV}$ found in the case where $M_1 \lesssim T_{\text{sph}}^{\text{out}}$. We have also described the transition between different fully flavoured regimes for a changing value of M_2 with a step approximation, while a full description would require solution of density matrix equations [11, 13, 39, 40]. Another important effect that we neglected and that might be important in the supersymmetric case for large $\tan \beta$ is the running of low energy neutrino parameters that might modify the constraints in this case [57]. However, this effect would not change our main results on the lower bound on T_{RH} . In conclusion, we have shown the existence of a window for the viability of thermal $SO(10)$ -inspired leptogenesis in the supersymmetric case without gravitino overabundance problem. Independently whether supersymmetry is found at the LHC, these results are interesting in connection with the current debate of identifying a realistic grand-unified model able also to realise successful leptogenesis, since supersymmetric extensions might more easily provide good fits of the parameters even if supersymmetry breaking occurs above the scale testable at colliders. With more experimental information on the neutrino mixing parameters coming in a close future, a particular successful model (or class of models) might emerge with interesting further phenomenological predictions (e.g proton life-time) and even more specific links between leptonic and quark sector and possibly with the identification of the DM candidate and new predictions at colliders. In this exciting search, leptogenesis might play a primary

role, increasing the predictive power of the model and solving the matter-antimatter asymmetry cosmological puzzle.

Acknowledgments

We thank Borut Bajc, Steve F. King, Luca Marzola and Rabi Mohapatra for useful comments and discussions. PDB acknowledges financial support from the NExT/SEPnet Institute, from the STFC Consolidated Grant ST/J000396/1 and the EU FP7 ITN INVISIBLES (Marie Curie Actions, PITN- GA-2011- 289442). MRF acknowledges financial support from the STAG Institute.

References

- [1] P. Minkowski, Phys. Lett. B **67** (1977) 421; T. Yanagida, in Proceedings of the Workshop on Unified Theory and Baryon Number of the Universe, eds. O. Sawada and A. Sugamoto (KEK, 1979) p.95; P. Ramond, Invited talk given at Conference: C79-02-25 (Feb 1979) p.265-280, CALT-68-709, hep-ph/9809459; M. Gell-Mann, P. Ramond and R. Slansky, in Supergravity, eds. P. van Nieuwenhuizen and D. Freedman (North Holland, Amsterdam, 1979) Conf.Proc. C790927 p.315, PRINT-80-0576; R. Barbieri, D. V. Nanopoulos, G. Morchio and F. Strocchi, Phys. Lett. B **90** (1980) 91; R. N. Mohapatra and G. Senjanovic, Phys. Rev. Lett. **44** (1980) 912.
- [2] M. Kado, ATLAS 13 TeV Results, CERN Jamboree (December 15 2015, <https://twiki.cern.ch/twiki/bin/view/AtlasPublic/December2015-13TeV>); J. Olsen, CMS 13 TeV Results, CERN Jamboree (December 15 2015, <http://cms-results.web.cern.ch/cms-results/public-results/preliminary-results/LHC-Jamboree-2015/index.html>).
- [3] M. Pietroni, Nucl. Phys. B **402** (1993) 27 [hep-ph/9207227].
- [4] M. Fukugita and T. Yanagida, Phys. Lett. B **174**, 45 (1986).
- [5] A. Y. Smirnov, Phys. Rev. D **48** (1993) 3264 [hep-ph/9304205]; W. Buchmuller and M. Plumacher, Phys. Lett. B **389** (1996) 73 [hep-ph/9608308]; E. Nezri and J. Orloff, JHEP **0304** (2003) 020 [hep-ph/0004227]; F. Buccella, D. Falcone and F. Tramontano, Phys. Lett. B **524** (2002) 241 [hep-ph/0108172]; G. C. Branco, R. Gonzalez Felipe, F. R. Joaquim and M. N. Rebelo, Nucl. Phys. B **640** (2002) 202 [hep-ph/0202030].

- [6] E. K. Akhmedov, M. Frigerio and A. Y. Smirnov, JHEP **0309**, 021 (2003).
- [7] H. Georgi, AIP Conf. Proc. **23** (1975) 575; H. Fritzsch and P. Minkowski, Annals Phys. **93** (1975) 193.
- [8] S. F. King, JHEP **1408** (2014) 130 [arXiv:1406.7005 [hep-ph]].
- [9] F. Feruglio, K. M. Patel and D. Vicino, JHEP **1509** (2015) 040 [arXiv:1507.00669 [hep-ph]].
- [10] P. Di Bari, Nucl. Phys. B **727** (2005) 318 [hep-ph/0502082].
- [11] R. Barbieri, P. Creminelli, A. Strumia and N. Tetradis, Nucl. Phys. B **575** (2000) 61 [hep-ph/9911315].
- [12] E. Nardi, Y. Nir, E. Roulet and J. Racker, JHEP **0601** (2006) 164 [hep-ph/0601084].
- [13] A. Abada, S. Davidson, A. Ibarra, F.-X. Josse-Michaux, M. Losada and A. Riotto, JHEP **0609** (2006) 010 [hep-ph/0605281].
- [14] O. Vives, Phys. Rev. D **73** (2006) 073006 [hep-ph/0512160].
- [15] S. Blanchet and P. Di Bari, Nucl. Phys. B **807** (2009) 155 [arXiv:0807.0743 [hep-ph]].
- [16] P. Di Bari and A. Riotto, Phys. Lett. B **671** (2009) 462 [arXiv:0809.2285 [hep-ph]]; X. G. He, S. S. C. Law and R. R. Volkas, Phys. Rev. D **78** (2008) 113001 [arXiv:0810.1104 [hep-ph]].
- [17] P. Di Bari and A. Riotto, JCAP **1104** (2011) 037 [arXiv:1012.2343 [hep-ph]].
- [18] P. Di Bari, L. Marzola and M. Re Fiorentin, Nucl. Phys. B **893** (2015) 122 [arXiv:1411.5478 [hep-ph]].
- [19] W. Buchmuller, P. Di Bari and M. Plumacher, Phys. Lett. B **547** (2002) 128 [hep-ph/0209301]; W. Buchmuller, P. Di Bari and M. Plumacher, Nucl. Phys. B **665** (2003) 445 [hep-ph/0302092]; G. F. Giudice, A. Notari, M. Raidal, A. Riotto and A. Strumia, Nucl. Phys. B **685** (2004) 89 [hep-ph/0310123]; A. De Simone and A. Riotto, JCAP **0702** (2007) 005 [hep-ph/0611357].
- [20] W. Buchmuller, P. Di Bari and M. Plumacher, Annals Phys. **315** (2005) 305 [hep-ph/0401240];
- [21] P. A. R. Ade *et al.* [Planck Collaboration], arXiv:1502.01589 [astro-ph.CO].

- [22] P. Di Bari and L. Marzola, Nucl. Phys. B **877** (2013) 719 [arXiv:1308.1107 [hep-ph]].
- [23] M. C. Gonzalez-Garcia, M. Maltoni and T. Schwetz, JHEP **1411** (2014) 052 [arXiv:1409.5439 [hep-ph]]; F. Capozzi, G. L. Fogli, E. Lisi, A. Marrone, D. Montanino and A. Palazzo, Phys. Rev. D **89** (2014) 093018 [arXiv:1312.2878 [hep-ph]]; D. V. Forero, M. Tortola and J. W. F. Valle, Phys. Rev. D **90** (2014) 9, 093006 [arXiv:1405.7540 [hep-ph]].
- [24] W. Buchmuller and M. Plumacher, Phys. Lett. B **511** (2001) 74 [hep-ph/0104189].
- [25] W. Buchmuller and M. Plumacher, Phys. Lett. B **511** (2001) 74 [hep-ph/0104189]; S. Blanchet and P. Di Bari, Nucl. Phys. B **807** (2009) 155 [arXiv:0807.0743 [hep-ph]]; F. X. Josse-Michaux and A. Abada, JCAP **0710** (2007) 009 [hep-ph/0703084].
- [26] S. Antusch, P. Di Bari, D. A. Jones and S. F. King, Nucl. Phys. B **856** (2012) 180 [arXiv:1003.5132 [hep-ph]].
- [27] P. Di Bari and S. F. King, JCAP **1510** (2015) 10, 008 [arXiv:1507.06431 [hep-ph]].
- [28] A. Dueck and W. Rodejohann, JHEP **1309** (2013) 024 [arXiv:1306.4468 [hep-ph]].
- [29] F. Buccella, D. Falcone, C. S. Fong, E. Nardi and G. Ricciardi, Phys. Rev. D **86** (2012) 035012 [arXiv:1203.0829 [hep-ph]]; G. Altarelli and D. Meloni, JHEP **1308** (2013) 021 [arXiv:1305.1001 [hep-ph]]; C. S. Fong, D. Meloni, A. Meroni and E. Nardi, JHEP **1501** (2015) 111 [arXiv:1412.4776 [hep-ph]]; A. Addazi, M. Bianchi and G. Ricciardi, arXiv:1510.00243 [hep-ph].
- [30] K. S. Babu and C. Macesanu, Phys. Rev. D **72** (2005) 115003 [hep-ph/0505200]; A. S. Joshipura and K. M. Patel, Phys. Rev. D **83** (2011) 095002 [arXiv:1102.5148 [hep-ph]].
- [31] M. Y. Khlopov and A. D. Linde, Phys. Lett. B **138** (1984) 265; J. R. Ellis, J. E. Kim and D. V. Nanopoulos, Phys. Lett. B **145** (1984) 181; K. Kohri, T. Moroi and A. Yotsuyanagi, Phys. Rev. D **73** (2006) 123511; M. Kawasaki, K. Kohri, T. Moroi and A. Yotsuyanagi, Phys. Rev. D **78** (2008) 065011 [arXiv:0804.3745 [hep-ph]].
- [32] M. Fujii and T. Yanagida, Phys. Lett. B **549** (2002) 273 [hep-ph/0208191].
- [33] H. Baer, S. Kraml, A. Lessa and S. Sekmen, JCAP **1011** (2010) 040 [arXiv:1009.2959 [hep-ph]].

- [34] N. Arkani-Hamed, S. Dimopoulos, G. F. Giudice and A. Romanino, Nucl. Phys. B **709** (2005) 3 [hep-ph/0409232].
- [35] S. Blanchet, D. Marfatia and A. Mustafayev, JHEP **1011** (2010) 038 [arXiv:1006.2857 [hep-ph]].
- [36] V. A. Kuzmin, V. A. Rubakov and M. E. Shaposhnikov, Phys. Lett. B **155** (1985) 36.
- [37] L. Covi, E. Roulet and F. Vissani, Phys. Lett. B **384** (1996) 169 [hep-ph/9605319].
- [38] M. Plumacher, Nucl. Phys. B **530** (1998) 207 [hep-ph/9704231].
- [39] R. Barbieri, P. Creminelli, A. Strumia and N. Tetradis, Nucl. Phys. B **575** (2000) 61 [hep-ph/9911315]; A. Abada, S. Davidson, F. X. Josse-Michaux, M. Losada and A. Riotto, JCAP **0604** (2006) 004 [hep-ph/0601083]; S. Blanchet, P. Di Bari and G. G. Raffelt, JCAP **0703** (2007) 012 [hep-ph/0611337]; A. De Simone and A. Riotto, JCAP **0702** (2007) 005 [hep-ph/0611357]; M. Beneke, B. Garbrecht, C. Fidler, M. Herranen and P. Schwaller, Nucl. Phys. B **843** (2011) 177 [arXiv:1007.4783 [hep-ph]]; P. S. Bhupal Dev, P. Millington, A. Pilaftsis and D. Teresi, Nucl. Phys. B **886** (2014) 569 [arXiv:1404.1003 [hep-ph]].
- [40] S. Blanchet, P. Di Bari, D. A. Jones and L. Marzola, JCAP **1301** (2013) 041 [arXiv:1112.4528 [hep-ph]].
- [41] C. S. Fong, M. C. Gonzalez-Garcia, E. Nardi and J. Racker, JCAP **1012** (2010) 013 [arXiv:1009.0003 [hep-ph]].
- [42] G. D'Ambrosio, G. F. Giudice and M. Raidal, Phys. Lett. B **575** (2003) 75 doi:10.1016/j.physletb.2003.09.037 [hep-ph/0308031]; L. Boubekeur, T. Hambye and G. Senjanovic, Phys. Rev. Lett. **93** (2004) 111601 doi:10.1103/PhysRevLett.93.111601 [hep-ph/0404038]; Y. Grossman, T. Kashti, Y. Nir and E. Roulet, JHEP **0411** (2004) 080 doi:10.1088/1126-6708/2004/11/080 [hep-ph/0407063]; M. C. Chen and K. T. Mahanthappa, Phys. Rev. D **70** (2004) 113013 doi:10.1103/PhysRevD.70.113013 [hep-ph/0409096].
- [43] P. Di Bari, Proceedings of the 39th Recontres de Moriond, 04 Electroweak interactions and unified theories: La Thuile, Aosta, Italy, Mar 21-28, 2004, [hep-ph/0406115].
- [44] S. Blanchet and P. Di Bari, JCAP **0703** (2007) 018 [hep-ph/0607330].

- [45] S. Antusch, P. Di Bari, D. A. Jones and S. F. King, Phys. Rev. D **86** (2012) 023516 [arXiv:1107.6002 [hep-ph]].
- [46] S. Yu. Khlebnikov, M. E. Shaposhnikov, Nucl. Phys. **B 308** (1988) 885;
J. A. Harvey, M. S. Turner, Phys. Rev. **D 42** (1990) 3344
- [47] G. Engelhard, Y. Grossman, E. Nardi and Y. Nir, Phys. Rev. Lett. **99** (2007) 081802
- [48] E. Bertuzzo, P. Di Bari and L. Marzola, Nucl. Phys. B **849** (2011) 521 [arXiv:1007.1641 [hep-ph]].
- [49] H. Fusaoka and Y. Koide, Phys. Rev. D **57** (1998) 3986 [hep-ph/9712201].
- [50] F. Capozzi, G. L. Fogli, E. Lisi, A. Marrone, D. Montanino and A. Palazzo, Phys. Rev. D **89** (2014) 093018 [arXiv:1312.2878 [hep-ph]].
- [51] J. Hamann, S. Hannestad and Y. Y. Y. Wong, JCAP **1211** (2012) 052 [arXiv:1209.1043 [astro-ph.CO]].
- [52] P. Di Bari, S. King and M. Re Fiorentin, JCAP **1403** (2014) 050 [arXiv:1401.6185 [hep-ph]].
- [53] M. Plumacher, Z. Phys. C **74** (1997) 549 [hep-ph/9604229].
- [54] M. Bolz, W. Buchmuller and M. Plumacher, Phys. Lett. B **443** (1998) 209 [hep-ph/9809381].
- [55] A. Arbey, M. Battaglia, L. Covi, J. Hasenkamp and F. Mahmoudi, Phys. Rev. D **92** (2015) 11, 115008 [arXiv:1505.04595 [hep-ph]].
- [56] V. A. Kuzmin, V. A. Rubakov and M. E. Shaposhnikov, Phys. Lett. B **155** (1985) 36.
- [57] K. S. Babu, C. N. Leung, J. T. Pantaleone, Phys. Lett. B **319** (1993) 191; S. Antusch, J. Kersten, M. Lindner, M. Ratz, M. A. Schmidt, JHEP **0503** (2005) 024.